Soft Matter

RSC Publishing

REVIEW

View Article Online
View Journal | View Issue

Protein–polyelectrolyte interactions

Cite this: *Soft Matter*, 2013, **9**, 2553

A. Basak Kayitmazer,[b] Daniel Seeman,[a] Burcu Baykal Minsky,[a] Paul L. Dubin[a] and Yisheng Xu†*[a]

The interactions of proteins and polyelectrolytes lead to diverse applications in separations, delivery and wound repair, and are thus of interest to scientists in *e.g.* (a) glycobiology, (b) tissue engineering, (c) biosensing, and (d) pharmacology. This breadth is accompanied by an assortment of contexts and models in which polyelectrolytes are seen as (a) protein cognates assisting in complex cellular roles, (b) surrogates for the extracellular matrix, mimicking its hydration, mechanical and sequestering properties, (c) benign hosts that gently entrap, deposit and tether protein substrate specificity, and (d) selective but non-specific agents that modify protein solubility. Unsurprisingly, this literature is somewhat segregated by objectives and paradigms. We hope this review, which emphasizes publications over the last 8 years, represents and also counterbalances that divergence. An ongoing theme is the role of electrostatics, and we show how this leads to the variety of physical forms taken by protein–polyelectrolyte complexes. We present approaches towards analysis and characterization, motivated by the goal of structure–property elucidation. Such understanding should guide in applications, our third topic. We present recent developments in modeling and simulations of protein–polyelectrolyte systems. We close with a prospective on future developments in this field.

Received 29th August 2012
Accepted 10th December 2012

DOI: 10.1039/c2sm27002a

www.rsc.org/softmatter

1 Introduction

Proteins and polyelectrolytes interact, primarily *via* electrostatics, to form complexes, which can have widely varied stoichiometries, architectures and phase states. To a considerable extent, these represent equilibrium systems and are thus amenable to numerous techniques of investigation. The biofunctionality of the proteins, apparently unperturbed under most conditions, has resulted in growing interest in the behavior of these complexes under laboratory and *in vivo* conditions. However, the remarkable estrangement between the disciplines of Protein Chemistry and this active and growing area prompts a glance at its historical roots.

From 1952 to 1955 Morawetz *et al.* published a series of papers on protein–polyelectrolyte complexes[1–4] which were cited with increasing frequency until 1963 and may have inspired similar studies by Alberty *et al.*[5] and others.[6,7] About half of these papers appeared in *J. Biol. Chem.*, *Biochem. J.* and *Arch. Biochem Biophys*. After 1961, citations to the Morawetz papers no longer appeared in biological journals, and in fact the field of protein–PE complexes was virtually dormant for the next two decades aside from the papers of V. Kabanov in *Vysokomol. Soedin.* and later studies by E. Tsuchida. Work along this line emerged above the radar in the mid 1990's in publications by Patrickios *et al.*[8] and Dubin *et al.*[9] along with increasing citations to Morawetz *et al.* During the subsequent "dark ages" less than 5 papers per year were published (statistics based on Web of Knowledge and Google Scholar), but the rate had essentially doubled by 2002. Since the last review in 2005(ref. 10) about 20 papers per year appear; and the overall annual citation rate for articles in this field is now 250, double that in 2005.

Justification for this current review comes not only from the doubling of citations, signifying continued interest, but also ongoing progress in methods of investigation. While none of these citations are found in the biologically oriented journals where Morawetz published, their broad relevance is demonstrated by their appearance in *J. Phys. Chem.*, *Langmuir*, *Macromolecules*, *Soft Matter* and (most notably) *Biomacromolecules*. This speaks for (1) their suitability for investigation from the standpoints of colloid physics, polymer science, physical chemistry, simulations, materials science, and engineering; (2) their manifold applications, established potential in food science, biomaterials, enzyme immobilization, protein purification, drug delivery and biosensors, all based on a wide variety of phase states; and (3) their potential relevance to biology. One of our hopes is to narrow the gap between material science and polymer physical chemistry, on the one hand, and biological chemistry on the other. We focus on the *ca.* 100 papers since our previous review.[10] Some of these have been noted in significant related reviews by Turgeon *et al.*[11] (primarily focused on food polysaccharides), Becker *et al.*[12] (particularly about spherical brushes), and de Vries and Stuart[13] and Ulrich *et al.*[14] (theory

[a]*Department of Chemistry, University of Massachusetts Amherst, MA 01003, USA. E-mail: yx276@cornell.edu*

[b]*Department of Chemistry, Bogazici University, Istanbul, 34342, Turkey*

† Current address: Materials Science and Engineering, Cornell University, Ithaca, NY 14850.

and simulations). Because of the unique complexity of certain food polysaccharides, such as gum Arabic, we have covered such systems in less detail. We specifically do not review the extensive literature on DNA-binding proteins, since those interactions are qualitatively different from those for random coil polyelectrolytes. On the other hand, we do describe the flexible chain glycosaminoglycans under "cognate systems", *i.e.* co-evolved protein–PE pairs whose interactions are biofunctional.

A broad range of experimental techniques makes it possible to establish the boundaries that define the existence of multiple states that result from protein–polyelectrolyte interactions. These techniques and their relevance for characterizing complexes are covered in the first part of the review, where we describe: turbidimetry, and light scattering (both static and dynamic); small-angle neutron scattering; calorimetry (primarily isothermal titration); microscopies – AFM, EM (including SEM and cryo-) and confocal; surface plasmon resonance and quartz crystal microbalance; Electrospray mass spectrometry; and capillary electrophoresis. Turning to the forces underlying protein–polyelectrolyte association, we discuss first (Section 3.1) the issue of protein charge anisotropy and its manifold and pervasive effects on protein–PE interactions. This is followed by a description of the states that arise from such interactions, covering (Section 3.2) the characterization of intrapolymer complexes and solution aggregates thereof; (Section 3.3) the structure and applications of protein–PE multilayers; (Section 3.4) the fundamental insights offered by studies of proteins in PE brushes; (Section 3.5) the utilization of responsive polyelectrolyte gels for modulating protein uptake and release; and (Section 3.6) the current understanding of protein–PE coacervates. Our next section deals with applications of protein–PE systems, and includes the stabilization and separation/purification of proteins with polyelectrolytes, protein delivery, and enzyme immobilization. Finally, we describe developments in simulation and theory that aim to account for particular features of complexes and complexation, including electrostatics and charge anisotropy, and polymer configurational dynamics.

2 Techniques of investigation

2.1 Light scattering

2.1.1 Turbidimetry. There is much potential confusion between the commonplace definition of "turbid" as the antonym of "clear", and the proper definition as $-\log T/b$, where b is the pathlength and T the transmittance, diminished by scattering. Since T can be measured to 1 ppt, "turbidity" should not be confused with opacity. Turbidimetric investigation of protein–polyelectrolyte complexation goes back at least to 1980 when Kokufuta and coworkers[15] applied the method of "colloid titration", in which one macroion is titrated to a turbidimetric (precipitation) end-point with another, to determine the stoichiometry of such complexes in pure water. "Stoichiometry" generally has the meaning of fixed combining ratio, but "stoichiometric titration" additionally connotes formation of detectable complexes with large association constants. "Stoichiometric end-points" could be identified as the point of protein:PE charge equality as long as the protein charge was large ($|\mathrm{pH} - \mathrm{p}I| \gg 1$) and opposite to PE, and titrations were done in pure water. Similar titrations in the presence of salts[16] showed that with diminution of the interaction energy, turbidity maxima might no longer show stoichiometric behavior, because phase separation (coacervation) could leave substantial amounts of macroions in the soluble phase. The drift away from stoichiometry upon increasing I beyond 1 mM, or decreasing $|\mathrm{pH} - \mathrm{p}I|$, signaled by both loss of abrupt transitions and end-point $[-]/[+] \ll 1$ was shown by Hiroshi *et al.*[17] for titrations of BSA with PVS. Boeris *et al.*[18] also found that turbidimetric end points, at $I = 50$ mM, drifted towards excess protein (chymotrypsin) ($([+]/[-])_{\text{end-point}} = 2$–5), even at $|\mathrm{pH} - \mathrm{p}I| > 5$. They attributed this to binding of one protein to each anionic PVS repeat unit, in contrast to the more reasonable range of 60–100 PVS repeat units/protein found by Matsunami *et al.*, who coupled turbidimetry (Fig. 1) with parallel static and electrophoretic light scattering measurements.

Maxima in turbidimetric titration curves are seen not only for a variety of macroion host–guest systems as a function of stoichiometry through degree of binding,[19,20] but also for protein–PE systems as a function of ionic strength[21] or pH.[22] It may be recognized that these last two variables also control charge stoichiometry, through the degree of binding and through macromolecular charges, so all of them may be conducive to charge neutralization. On the other hand, Tikhonenko *et al.*[23] attributed turbidity maxima in the titration of urease with polyallylamine by salts to aggregation of the PE–protein complex, which is enhanced by a form of salting out, followed by dissolution with excess polycation.

Turbidity invariably accompanies coacervation, but the distinction from precipitation is not always clear; without centrifugation it may be difficult to distinguish metastable liquid/liquid *vs.* liquid/solid suspensions. Coacervation is a true

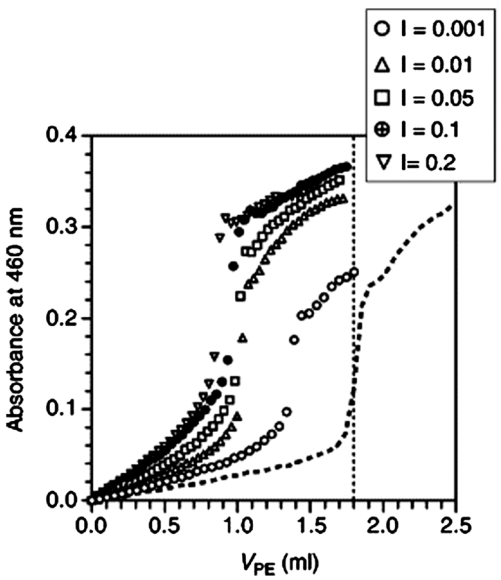

Fig. 1 Results of turbidimetric titration of BSA with KPVS during the titration process. The titration was performed at pH 3 and at different ionic strengths (I) (see plots), as well as at pH 2 and $I = 0.001$ (broken line).[17]

liquid–liquid phase transition: an abrupt and reversible increase in τ can be observed if system polydispersity is low, and the critical point is approached in an equilibrium manner, but these two requirements are often lacking due to the heterogeneity of protein and/or PE, or due to simple mixing which establishes irreversibility from pH or concentration gradients.

An essentially equilibrium form of turbidimetric titration, involving addition of a strong base or acid at fixed I and macromolecular concentrations, leads to identification of more subtle transitions. While turbidity is popularly equated with opacity, the proper definition of turbidity $\tau = -\ln T/x = 2.3A/x$ – where T is the transmittance, A the absorbance, and x the path length (cm)[24] – shows that measurements of optical density with ± 0.001 precision can yield τ with sufficient sensitivity (*i.e.* $\pm$ 0.02% T) to detect *e.g.* protein dimerization. It is possible then to observe, with a simple probe colorimeter and modest signal averaging, the departure from zero slope in the turbidity as a function of pH that corresponds to the onset of protein–PE complexation. This operational definition of "pH_c" has been accepted as an indication of a pseudo-phase transition, which presumably corresponds to the point at which cooperative binding of some contiguous set of PE segments provides an energy > kT. Somewhat less demanding is the determination of "pH_φ", the onset of coacervation.

Turbidimetry can be used to measure protein aggregation in the presence and absence of a polyelectrolyte.[18,25] The primary difficulty here is the incorporation of $d\tau/dt$ in kinetic expressions since it does not represent the consumption of the "reactant" (unaggregated protein), but rather corresponds to the formation of what may be an ill-defined aggregate. $\tau(t)$ may exhibit apparent first-order behavior,[26–28] *i.e.* $\tau = \tau^{\text{terminal}}(1 - e^{-kt})$ but interpretation may be limited to nucleation and growth aggregation mechanisms established by a linear dependence of τ^{terminal} on protein concentration.[27] The effect of PE on $d\tau/dt$ is of considerable interest for PEs in aggregation inhibition by PEs, but the combination of complex equilibrium with aggregation kinetics can be difficult to deconvolute.

2.1.2 Static light scattering (SLS). SLS of protein/PE soluble complexes can yield quantitative information on both molecular weight and dimensional parameters including fractal dimension and radius of gyration (R_g) depending on the size of the particle in relation to the available q-range. However, mixtures of proteins and PEs can form very complex and/or heterogeneous systems and the absolute molecular weight can be determined only under some limiting conditions. In some cases, only intensity at a single angle is used, in contrast to multiple angle measurements. Since scattering intensity at a single angle is proportional to both molecular weight and concentration, such measurements can be used to follow the growth of particles, similar to turbidity. In these instances SLS is usually coupled with other scattering techniques such as small-angle scattering, DLS, turbidity, or in some cases with non-scattering based techniques.

SLS can be used quantitatively to analyze multi-component protein–PE complexes (despite the notable absence of Zimm plots presentations). PE microgels were characterized by multiangle static light scattering measurements, where the weight average molecular weight (M_w) and R_g of each microgel were determined at low q.[29] The change in complex M_w coupled with swelling was used to assess the amount of protein loaded.[29] The gelation of native BLG with xanthan gum was followed by SLS, where a higher order structure was observed.[30] Small-angle SLS was used to study BLG–xanthan gum mixtures under shear, where the measurement of the fractal dimension of the resulting complexes was coupled with turbidity-like methods to infer a mechanism of phase separation. The complexes were found to initially form diffuse structures and then gradually condense into denser aggregates.[31] Coacervates of BSA and PDADMAC were studied by SLS in order to obtain R_g values of the dense domains within the coacervate; these dense domains were found to have strong scattering and show little influence of salt.[32]

Extrapolation to zero concentration is clearly problematic for determination of parameters such as M_w. However, it is still possible to take intensity to be proportional to M_w at a given angle, allowing one to qualitatively study size changes. The assembly, swelling, and BSA loading in soluble nanoparticles formed from BSA and anionic graft copolymers were inferred from changes in scattered light at 90°, as both a function of weight percent of reactants and solution pH.[19] The analysis of these nanoparticles was also facilitated by comparing R_g obtained from SLS, with R_h from DLS, the ratio R_g/R_h yielding information on the form of the particles.[19] Similarly, the temporal evolution of scattering intensity of mixtures of BLG and xanthan gum was followed at a single angle, and the results were used to infer a nucleation and growth mechanism for complex phase separation.[31]

2.1.3 Dynamic light scattering (DLS). DLS is a primary tool of investigation, reported in 35% of the papers published since the last review. The multiple modes typically observed have usually been attributed to the unbound protein, intrapolymer complexes, and interpolymer complexes (soluble aggregates). In the case of protein–PE coacervates, DLS yielded the first evidence of what appeared to be an anomalously fast diffusional mode, subsequently linked *inter alia* with equilibrium mesophase organization;[32,33] the relationship of such structures to those at incipient coacervation is still under investigation.[34] With regard to solution structures, complexation of chitosan (R_h = 400 nm) with pepsin ($pI = 1.0$) at pH 3.0 did not alter this size, while complexation at pH 4.0 reduced it by a factor of two. This was attributed to neutralization of chitosan charge by the more strongly bound and more negative protein at higher pH.[35] A smaller compression of dimensions of an isopropylacrylamide/NaPSS copolymer upon binding soybean peroxidase was reported, further enhanced with temperature presumably due to enhanced hydrophobic interactions.[36] However, R_h as a function of temperature attained a minimum *ca.* 50 nm, this complex behavior attributed to simultaneous collapse and association.

The foregoing small sample indicates the diverse applications of DLS but should be accompanied by some caveats. Confidence has grown regarding the interpretability of multiple modes, but this relies on the robustness of the autocorrelation software. Signals from smaller but more abundant species may be obscured by strong scatterers. Fast modes due to PE chain

motions may be difficult to discern from free protein dynamics; slow modes may not correspond to large objects and repulsive interactions at low salt concentrations may lead to anomalously "fast" decays. Some of these issues are addressed by establishing whether modes are in fact diffusional, but Stokesian assumptions confront the enigma of "local viscosity".

2.2 Small-angle scattering

Small-angle scattering techniques such as small-angle neutron scattering (SANS) lead to characteristic dimensions and structures of protein–PE complexes at length scales inaccessible by static light scattering techniques. As SANS is capable of accessing a wider range of q-values than light scattering, it allows for direct measurement of such structurally complex systems. The effectiveness of various PE–protein systems in loading or releasing protein can be quantitatively assessed. Finally, appropriate choice of the model can give information on the form of a particular system, especially in differentiating simple globules, chains, and fractal aggregates.

2.2.1 Mechanistic details of the lysozyme–PSS system. Complexes between lysozyme and the negatively charged polyelectrolyte PSS were thoroughly characterized over an expansive range of accessible length scales by Gummel and coworkers using SANS.[37] Contrast matching conditions were determined in order to "see" either lysozyme, PSS, or whole complexes, allowing determination of the fractal dimensions of individual constituents.[38] Initially a fractal dimension of 2.1, consistent with reaction limited aggregation (RLA), was determined for these complexes.[37] Additionally, it was reported that the fractal dimension mentioned above persisted even after systematic dilution of complexes suggesting no major perturbations once complexation occurs, despite subsequent concentration changes.[39] Further SANS studies of lysozyme–PSS gave insight into the structural hierarchy within such complexes suggesting reorganization of the complexes at some length scales.[39] Scaling/power laws were interpreted across a range of length scales in order to assess interfaces, ordering, and hierarchy of protein–PE complexes.[40] The size, structure, and composition of highly turbid lysozyme–PSS complexes were obtained and the mechanism was found again to be consistent with RCLA in all respects.[41] Furthermore the structure of protein–PE complexes is entirely consistent with features observed by microscopy over the length scales where the complex structure persists. This suggests that coverage of length scales from nm to micron sized is possible with one technique.[41]

2.2.2 Quantitative use of SANS. Analysis of the composition of complexes is also achieved through analysis and interpretation of volume fractions of either the protein or solvent. SANS has proved useful in characterizing the release behavior of the protein lipase from polyelectrolyte vesicles, by allowing determination of the volume fraction of the protein confined within a typical vesicle.[42] Analysis of the protein content within the vesicle shows that increase of ionic strength gradually diminishes repulsive interactions between the cationic vesicles and target protein. Further increase of I beyond 120 mM completely screens electrostatic attractions and all protein is released.[42] Volume fraction determination was used to evaluate equilibrium interactions between anionic pectin and cationic lysozyme, yielding quantitative measurements of water content.[43]

2.2.3 Model-dependent fitting. Appropriate structural or chain models allow for precise determination of model parameters, and conformational properties of PE–protein systems can also be obtained. A significant reduction in the apparent persistence length of PSS was observed upon interaction with lysozyme when scattering was fit to a semi-flexible worm-like-chain model.[44] Schmidt *et al.* studied foam thickness by assuming a biphasic system with a well-defined surface or interface.[45] Chodankar *et al.* observed two discrete length scales in BSA–PSS mixtures at conditions of phase separation by fitting the scattering data to an empirical model.[46] Lindhoud and coworkers found high internal water content and a stoichiometry of two proteins per micelle in lysozyme-filled PE micelles by fitting their scattering data to a core shell model.[47] The extended rod-like structure formed by complexes of hyaluronan and lysozyme displayed different levels of extension and rigidity depending on the −/+ charge ratio as shown by Morfin and coworkers.[48]

In contrast to more elaborate models, simple scaling laws themselves based on a series of assumptions can also yield structural parameters, including R_g and d_f. When applied to the study of BSA and anionic graft copolymers these simple models can yield R_g.[19] The study of BSA–PSS complexes over a range of conditions shows an increasing fractal dimension showing the formation of more dense complexes as protein pI is approached.[46]

2.3 Isothermal titration calorimetry (ITC)

ITC provides quantitative measurements of the thermodynamics of protein–PE interactions from which the nature of the interaction could be explored.[49] The resultant binding isotherms have implications for complex structures, since binding equilibrium is viewed as a binding isotherm determined from ITC. The raw thermogram directly is comprised of enthalpy changes (ΔH°) at different protein–PE stoichiometries. In the first injection where titrant is completely bound to substrate, ΔH° may reflect the binding affinity between the protein and PE.[50–52] Fitting the binding isotherm with appropriate binding models gives the binding constant (K_b) and number of proteins bound per PE chain.[53] ΔH° and ΔG° are combined to yield ΔS° as shown in Fig. 2.[54] Analysis of these parameters allows for evaluation of possible driving forces of protein–PE interactions.[54] Both electrostatic and hydrophobic interactions can be exothermic. Hence exothermic processes in the absence of hydrophobic interactions can usually be seen as driven by electrostatics. For example, Karayianni studied the interactions between lysozyme and poly(sodium(sulfamate-carboxylate) isoprene) and deduced strong electrostatic interactions between PE and protein as evidenced by large exothermic injections.[55] Romanini and Braia confirmed the electrostatic nature of PE–protein interactions for lysozyme–polyanions (polyacrylic acid (PAA) and polyvinyl sulfonic acid (PVS))[56] and trypin–PVS[57] systems by showing exothermic

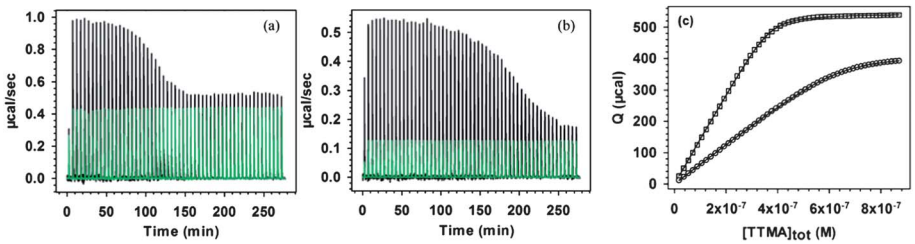

Fig. 2 ITC raw data for the interaction of (a) BLGATTMA and (b) BLGBTTMA at pH 5.5 and $I = 5$ mM. Green lines mean a control experiment in which BLGA/B was diluted by a buffer under the same condition. (c) Binding isotherms for (□) BLGA-TTMA and (○) BLGB-TTMA from the integration of the curves in (b) and (c).[54]

processes and negative entropy terms. They further found that more heat was released with the strong PE (PVS) suggesting stronger electrostatic interactions than for the weak PE (PAA).[56] In addition to electrostatic interactions, their studies on the anionic polyelectrolyte Eudragit® L100 show that additional hydrophobic groups can lead to significant contributions.[58] However, several ITC studies indicate that the entropic driving forces for protein adsorption on charged interfaces or polymeric layers is due to counterion release. Welsch *et al.*[59] also showed by ITC that the binding of lysozyme to a negatively charged microgel is an entropically driven process, although evidence for electrostatic interactions also comes from the ionic strength dependence of binding affinity. Henzler *et al.*[60] reported entropically driven interactions between BLG and 100 nm negative spherical polystyrene brushes due to counterion release. Similar ITC results by Becker *et al.* indicated that the adsorption of RNase A on cationic polystyrene PE brushes is also due to counterion release.[61] In summary, the details of PE–protein interactions may be difficult to ascribe to a particular mechanism, but ITC provides an efficient way to understand their thermodynamics.

2.4 Surface plasmon resonance (SPR)

Compared with other techniques such as fluorescence labeling, SPR allows for the observation of protein–PE adsorption kinetics on surfaces without the requirement of protein labeling. Due to its high sensitivity to refractive index changes, SPR has been widely used to measure the kinetics of adsorption of proteins on PE-treated surfaces,[62] or PEs on protein-modified surfaces,[63] and SPR has also been employed in sensors. The binding isotherms at different concentrations can easily be deduced from the binding kinetics to obtain binding constants.[64] Kusumo *et al.* studied selective kinetic adsorption of BSA on poly(2-(dimethylamino)ethylmethacrylate) (PDMAEMA) brushes on gold.[65] As examples of sensors, Kim *et al.* fabricated a poly(diallyldimethylammoniumchloride) coated array for a high-throughput biosensor of mumps virus from 0.5×10^5 to 14×10^5 pfu mL^{-1}.[66] Vaisocherová reported a zwitterionic poly(carboxybetaineacrylamide) biomimetic material as a unique biorecognition coating with an ultra-low fouling background, enabling sensitive and specific detection of proteins in blood plasma.[67] Interestingly, SPR has also been used to study pH induced conformational transformation of poly(acrylic acid)–BSA complexes at $3 < pH < 5$. The SPR signal increases with decreasing pH indicating the increase of refractive index as the complex becomes insoluble, and thus more compact.[68]

2.5 Quartz crystal microbalance (QCM)

The mass information obtained from QCM closely resembles that from SPR. A QCM can detect mass changes of the order of nanograms per cm^2.[69] Instead of monitoring refractive index change, QCM is based on a different transducer mechanism depending on the frequency change (Δf) of a shear-oscillating piezoelectric sensor when analytes bind to the functionalized sensor.[70] In order to accurately measure the mass adsorbed, three criteria should be fulfilled: (1) the adsorbed mass must be small compared with the mass of the crystal sensor; (2) the materials adsorbed must be rigid; (3) the mass adsorbed must be evenly distributed on the surface. Therefore, QCM is often used to monitor the kinetic assembly of PE multilayers and protein adsorption in/on these layers; the corresponding surface coverage can be calculated.[69,71–77] However, since PE–protein systems are not rigid, the relationship between Δf and Δm is no longer accurate. This leads to QCM-D, an improvement of QCM which provides not only Δf but also changes in energy dissipation D. Further structural information such as softness of adsorbed materials can then be obtained. As an example of QCM-D, Kepplinger *et al.* calculated the thickness of a cytochrome C/poly(aniline sulfonic acid) multilayer with different overtone frequencies and found similar thickness to prove the rigidity of such layers.[78] The constant or small dissipation values can be the basis for precise calculation of mass change as shown by Gormally *et al.*[79] and Delcea *et al.*[80] Otherwise, a change in dissipation values should indicate some change of softness of the mass adsorbed. Hamlin found that a β-galactosidase film adsorbed on multilayers became more rigid with time which was consistent with the trend of mass increase with time.[81] Delcea *et al.* showed that the combination of QCM-D with AFM and neutron-reflectometry allowed estimation of the thickness of a loosely packed S-protein layer on PE multilayers.[80] Martins *et al.* observed a relatively soft HSA layer in chitosan/alginate multilayers by QCM-D.[82] Borges *et al.* reported the concentration dependence of rigidity of a BLG layer adsorbed on chitosan, *i.e.* the protein layer becomes relatively soft as the concentration exceeds 25 μg mL^{-1} at $I = 0.05$ M and $pH = 5.5$.[83]

Mass measurements by QCM correspond to the total mass related to the movement of the sensor including the mass of molecules adsorbed on the surface and the water entrapped in these molecules. This technique has been used to measure the

water content of surface layers when coupled with SPR, which only measures the dry mass adsorbed on the surface.[84] Bittrich *et al.* studied the considerable hydration of BSA adsorbed on PAA Guiselin brushes leading to swelling of the brush layer in the electrolyte solution by QCM-D.[85]

2.6 Microscopy

Microscopy including AFM, EM and confocal microscopy has been widely and routinely used for the study of morphology or dynamics of protein–PE complexes on flat substrates.

2.6.1 AFM. AFM is one of the most common techniques used to characterize topology of PE–protein surfaces with nanoscale resolution.[73,75,83,86–89] The average roughness (rms) can be used to qualitatively monitor PE–protein adsorption on surfaces. Moreover, the 3-dimensional features of large particles adsorbed on a surface can be quantitatively determined.[50,90–93]

Force–distance curves determined by AFM can be used to study protein adsorption and surface softness since protein-bound surfaces are more attracted to the AFM tip than to the unbound surface.[94] Delcea *et al.*[80] found that the denatured S-protein on surfaces showed softer structures than the native protein by analyzing the force–distance curve. In the same way Olanya *et al.*[95] found stronger attraction between the AFM tip and lysozyme for low charge density PE multilayer surfaces. This indicates more protein adsorption due to decreased charge–charge repulsions for low charge density surfaces.

2.6.2 Confocal Laser Scanning Microscopy (CLSM). CLSM can control the depth of the scanning field and eliminate the light from the focal plane, and thus measure the signal from a series of sections of a thick sample compared with conventional epi-fluorescence microscopy.[96] Moreover, removal of out-of-focus light enhances the resolution of this technique relative to conventional fluorescence microscopy. Therefore, CLSM is a very common method in *in vivo* studies to localize proteins in different tissue depths.[97] CLSM is also widely used to image protein distributions or their diffusion on PE-surfaces[98,99] or in PE–protein capsules,[99–102] gels,[103] coacervate[104] or particles.[105] For example, Crouzier *et al.* observed the diffusion of recombinant human bone morphogenetic protein 2 inside a poly(lysine)–hyaluronan multilayer film from the concentration gradient of protein along the *z*-direction.[106] Johansson *et al.*[107] observed an even distribution of lysozyme in poly(acrylic acid)/lysozyme microgels at low concentrations, but diffusion of protein to the outer shell at high concentration. Li *et al.*[108] quantitatively studied the time dependent release of lysozyme from hydrogels by CLSM. They further investigated the effect of PE multilayer coating on the release kinetics of proteins from the same hydrogel.[109]

2.6.3 Electron microscopy (EM). In electron microscopy, an electron beam illuminates samples which are often stained to improve contrast. This technique provides much higher resolution than optical microscopy as electrons have wavelengths about 100 000 times shorter than visible light. EM is widely used to study sample morphology, composition, and crystallinity. EM is widely used to study sample morphology, composition, crystallinity, and also to characterise protein–PE and PE–PE complexes.[110–115] Transmission electron microscopy (TEM) when coupled with cryo techniques, has been used to understand the structure of PE–protein complexes. Gummel reported dense spherical structures formed by polyelectrolyte–protein complexes by cryo-TEM. This dense domain in protein–PE complexes was also found by Kayitmazer *et al.*[32] for the BSA–PDADMAC system using cryo-TEM. They further observed 50 nm aggregates of BSA–PDADMAC complexes at higher resolutions.[33]

2.7 Mass spectrometry

Mass spectrometry is not usually used to study protein–PE systems due to their complexity. However, PEs can be used for selective enrichment of analytes or directly as a matrix for laser desorption/ionization mass spectrometry (MALDI). PEs have been recently developed to preconcentrate or to fractionate protein/peptide samples for MALDI analysis. For example, Rodthongkum *et al.* have applied reverse micelles, formed by a new type of amphiphilic homopolymer, to selectively enrich protein or peptide biomarkers by choosing an appropriate p*I* cutoff followed by MALDI analysis.[116,117] This technique can achieve reproducible analysis with detection limit as low as 10 fM.[116] Dunn *et al.* reported efficient enrichment of phosphopeptides by poly(2-hydroxyethyl methacrylate) (PHEMA) brushes prior to MALDI analysis.[118] A modified PE film can replace the traditional small molecule matrix used for protein analysis.[119] PE films provided several advantages over organic molecule matrices: (1) the addition of a matrix step is no longer necessary; (2) the resolution is increased due to the elimination of ionization of small molecules as the PE is covalently bonded on the surface.[119] Lbl self-assembled multilayers made of gold nanoparticles (AuNPs) on silicon wafers have been successfully used for insulin and cytochrome c analysis.[120]

2.8 Capillary electrophoresis

Capillary electrophoresis (CE), through measurement of the mobilities and concentrations of free and bound ligands, is a powerful tool for investigating protein–polyelectrolyte interactions. The modes of analysis include capillary zone electrophoresis (CZE), affinity capillary electrophoresis (ACE), the Hummel–Dreyer method (H–D), and frontal analysis continuous capillary electrophoresis (FACCE). In CZE, separation efficiency is highly correlated with injection time, capillary conditioning, capillary length and mobile phase flow rate.[121] The peak areas or the peak heights of the distinct plateaus, representing a free ligand or complex, can be used to calculate binding parameters. CZE was employed to calculate binding constants between low molecular weight heparin–interleukin 2 (IL-2)[122] and heparin-programmed cell death 5 (PDCD5) protein.[123]

The Hummel–Dreyer method, or its equivalent ACE, can be used to examine dynamic equilibria between substrate and the ligand. The substrate is injected into the ligand-containing buffer, and binding affinities can be calculated from the shifts in the electrophoretic mobility – due to substrate–ligand interactions – as a function of free ligand concentration.[124] In this analysis, the differences between the successive complex

mobilities are assumed to increase incrementally. Therefore, as discussed by Winzor, the calculation of binding stoichiometry remains a problem.[125] ACE has been widely used to calculate binding constants in biological polyelectrolyte–protein systems including heparin and the heparin-binding domain of amyloid precursor protein (APP),[126] heparin–human β2-glycoprotein[127] and non-cognate pairs such as fucoidan–Antithrombin (AT),[128] sulfated lignins–AT,[129] heparin/dextran sulfate–BSA and Ribonuclease (RNase).[130]

The continuous injection mode, FACCE, provides robust quantitation of protein–polyelectrolyte interactions. FACCE facilitates determination of free and bound ligand concentrations without perturbing the binding equilibrium, and compared to CZE and ACE, is applicable to slow binding kinetics. In FACCE,[131] the capillary is first equilibrated with the run buffer, then the sample and the buffer vials are placed in the inlet and outlet ends, respectively. The protein–polyelectrolyte mixture is injected continuously under a constant voltage, and the unbound protein (first plateau) and the complex (second plateau) can be determined quantitatively. This methodology is analogous to ascending an electrophoretic pattern, the separation of a fast solute boundary from the original reaction mixture.[132] However, as stated by Winzor, FACCE can only determine binding data for systems and complexes co-migrate more rapidly than reactants (polyelectrolyte) migrate.[133] Control experiments should be conducted to validate these requirements. FACCE was first used to measure (BLG–NaPSS) the binding parameters (Fig. 3).[131] The McGhee–von-Hippel overlapping binding sites model was used to determine cooperativity, intrinsic binding constants, and sizes of the binding site.[134] Hattori *et al.* similarly used binding isotherms, to determine the binding constant and binding site size for the BSA–Hp.[134] Seyrek *et al.* obtained the binding isotherms for cognate AT–heparin system using FACCE and showed that maximum binding occurs at $5 < I < 30$, where the Debye length is close to the radius of the protein.[135] Saux *et al.* used both ACE and FACCE to calculate the binding constants between AT and different molecular weight heparin fragments.[136] Fermas *et al.* successfully coupled FACCE and ESI-MS for the online analysis of AT–pentasaccharide complexes.[137]

2.9 Circular dichroism spectroscopy

Circular dichroism (CD)[138] has been used to assess protein secondary or tertiary structures before, during, and after complexation with polyelectrolytes.[105,107,113,138–142] Since folded globular proteins have unique CD signatures in their native states, this can be a convenient method for evaluating the retention, loss, or alteration of protein structure. CD can be used to confirm retention of protein structure[113] in the complexation process,[139] and is also particularly useful in assessing the integrity[107,140] of proteins in delivery and release applications.[105,141,142]

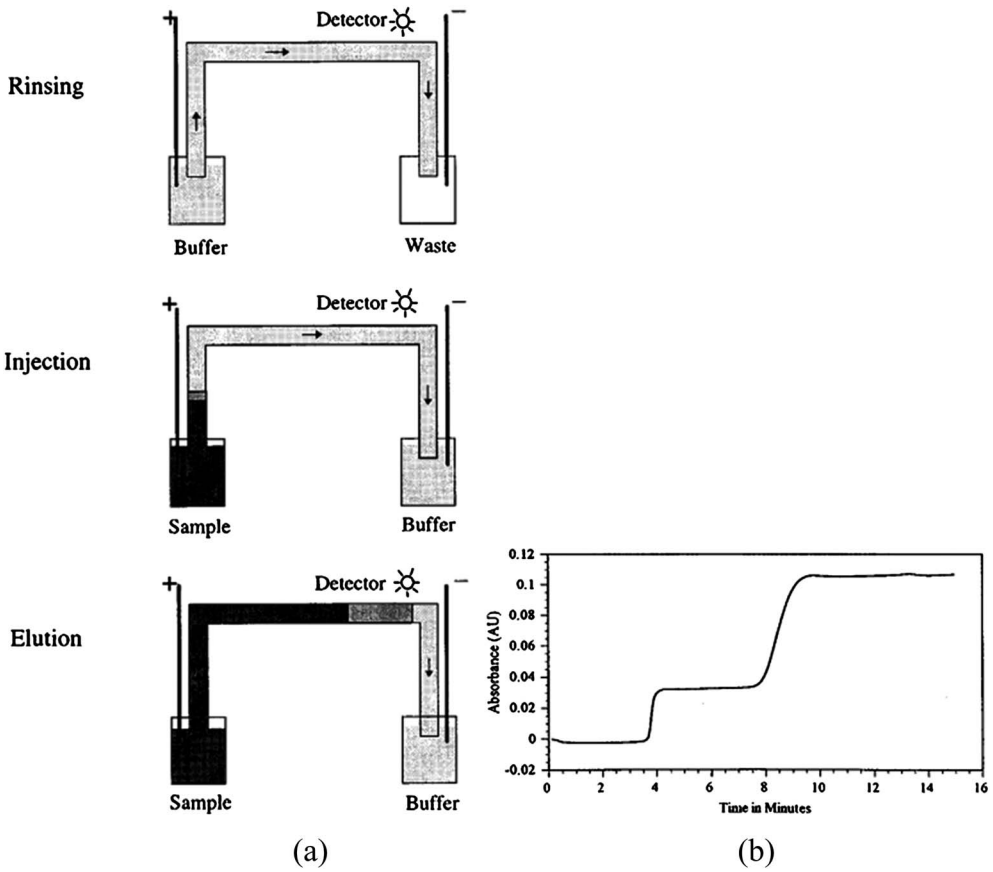

Fig. 3 (a) Schematic of FACCE. (b) Typical electropherograms obtained with 1.0 g L^{-1} β-lactoglobulin + 0.2 g L^{-1} NaPSS. Run buffer: 0.05 M phosphate at pH 6.7.[131]

2.10 Fluorescence spectroscopy

Fluorescence spectroscopy encompasses many techniques including fluorescence anisotropy/polarization, intrinsic protein fluorescence, as well as Fluorescence (or Förster) Resonance Energy Transfer (FRET) techniques. Within the context of protein–PE complexation, fluorescence anisotropy can be useful in that a fluorophore-tagged protein will have a very different rate of rotation when bound to a polyelectrolyte. For these cases the change in fluorescence anisotropy as a function of PE concentration can be used to construct a binding isotherm for cases where fluorescence anisotropy is believed to correlate with complexation.[143] In addition it provides information about the rotational freedom of a fluorophore-tagged protein within a protein–PE complex.[144] Intrinsic protein fluorescence, in which the fluorescence of residues such as tryptophan present within many proteins, is used as a reporter of protein chemical environment. Either the magnitude of emission intensity or shift in wavelength of maximal emission intensity can probe complexation.[144] In FRET, transfer of fluorescence between a donor and acceptor molecule can semi-quantitatively evaluate the average distance between the two probes within a particular protein–PE complex.[145]

2.11 Size exclusion chromatography (SEC)

Size exclusion chromatography, also called gel filtration, molecular-sieve or gel permeation chromatography, is a versatile analytical technique for purification or characterization of protein–ligand complexes. In zonal chromatography mode SEC is widely used to determine the apparent sizes of the protein–ligand complexes based on calibration curves that relate hydrodynamic radii to elution volumes. In this way, Tao and Zhang calculated the size of the protein–polysaccharide complexes extracted from the sclerotia of *Pleurotus tuber-regium* using preparative SEC with an ultraviolet absorbance (UV) detector, and analytical SEC with laser light scattering (LLS), refractive index (RI) and UV detectors to obtain molecular weight, radius of gyration and polydispersity (M_w/M_n).[146]

Frontal (large-zone), and Hummel–Dreyer methods can be used to determine macromolecule–ligand binding constants. As discussed by Winzor, frontal analysis differs from zonal chromatography only in the large sample volume, which guarantees that the elution profile exhibits a plateau region.[125] Because migration is dominated by size, the complex migrates faster than the free ligand, and the concentration of the complex and the free ligand can be obtained from the plateau heights, which are then used to calculate binding constants. The disadvantageous requirement of the large protein–ligand volume is addressed by the Hummel–Dreyer method, applicable to systems that are dynamic and equilibrate faster than the chromatography run time.[147] A small zone of the protein–ligand mixture is applied to the column, which is pre-equilibrated with a known concentration of ligand. The injected ligand concentration is varied, and the amount of free ligand can be deduced from the area of the negative peak. For example, Xia and Dubin ascertained the number of lysozymes bound per poly(dimethyldiallylammonium chloride) chain.[148] Complex stoichiometry can also be evaluated from the apparent molecular weights or the sizes of the complexes, which are calculated from the calibration curve. Complex peaks can also be analyzed using SEC with mass spectrometry. Robinson *et al.* calculated the sizes of FGF1–FGFR2–heparin oligomer (dp6–dp12) complexes and obtained a 2 : 2 : 1 stoichiometry.[149] Harmer *et al.* detected the multimers of FGF and FGFR on long heparin chains using offline SEC/MS, and observed 2 : 2 : 1 and 4 : 4 : 1 FGF–FGFR–heparin complexes.[150]

2.12 Viscoelastic measurements of protein–polyelectrolyte complexes

Viscometry, rheology and quartz crystal microbalance analysis have been used to determine viscosities or viscoelastic properties of protein–polyelectrolyte systems. Park *et al.* applied viscometry to protein-loaded polyelectrolyte complexes (PECs) to observe the relation between PEC viscosity and protein release efficiencies.[151] Rheology, which measures the flow characteristics of a substance under an applied stress, is mostly used to characterize gels and coacervates. Bohidar *et al.* applied rheology to probe the dynamics of BSA–PDADMAC coacervates, for which they observed a tenuous network, solid-like at low strain, but reforming after breakage by shear.[152] In food colloids, rheology has been used to study the effects of salt concentration and protein–polysaccharide ratio (BLG–pectin)[129] on the network structure of complex coacervates (agar–gelatin),[153] and to examine the kinetics of electrostatic gelation (native BLG–xanthan gum).[30] (For more examples, see Section 2.12.) Rheology was employed by Antonov and Moldenaers to characterize the structure and droplet morphology of sodium caseinate–sodium alginate water-in-water emulsions.[115] The mass and viscosity of protein–PE complexes on surfaces or within the thin films can be measured using a quartz crystal microbalance (QCM). The change in shear viscosity upon BSA adsorption on polyacrylic acid (PAA) brush surfaces was investigated by Bittrich *et al.* using coupled spectroscopic ellipsometry–quartz crystal microbalance with dissipation (QCM-D).[85] (For more examples, see Section 2.5.)

3 States

3.1 Protein charge anisotropy: the charge patch

Polyelectrolytes would not interact electrostatically with proteins of the same net charge unless they had anisotropic charge distribution. And yet this does happen, even biofunctionally for heparin-binding proteins, and the ionic strength dependence confirms that in general such "charge patch" interactions are not driven by hydrophobic effects. Among all the areas covered in this review, no single concept is as ubiquitous as the "charge patch". This term encompasses many ways of viewing protein charge anisotropy, and the 900 papers containing this phrase reveal a wide range of definitions, or their absence. The general concept of a protein region with a local charge density differing from or – more significantly – opposite to the global charge appears to have first arisen from protein retention in ion-exchange chromatography at the

"wrong side of p*I*" (or equivalently on the "wrong" type of column). The implication that the interaction, although electrostatic, is not governed by global charge was pointed out by Regnier *et al.*[154] Lesins and Ruckenstein then examined the ionic strength I and pH dependence of the strength of the protein–column interaction (capacity factor, k') for four proteins on an anion-exchange column as shown in Fig. 4, and reached three perceptive conclusions:[155] (1) the value of k' reflects both repulsion and attraction, the former shown by its direct dependence on I, the latter by an inverse dependence; (2) dominance of the attractive part at pH $\cong$ pI is evidence of a negative patch protein (*e.g.* ribonuclease at pH < pI on this positively charged column); and (3) the patch contains amino acids with pKs in the same range of pH where attraction changes to repulsion. Strege *et al.* also found that the tendency of proteins to phase separate (coacervate) with a synthetic polycation did not correlate with net protein surface charge density: in 100 mM salt, coacervation could occur below pI ("wrong side") for lysozyme and trypsin, but only above pI for serum and egg albumin; the inference was that local concentrations of negative charge promoted the binding of the first two basic proteins.[156] These were by no means the earliest observations of "inverted binding"; in fact Morawetz and Hughes in 1952 reported without comment that the polyanion poly(methacrylic acid) could precipitate BSA (pI 4.9) at pH 5.2 in pure water.[1] Heparin, the most highly charged of all natural polyanions, was known for many decades to bind avidly antithrombin at pH 2 units above the pI, but even the fact that chemical neutralization of lysine residues in general prevent binding[157] was deemed irrelevant in 1978. That this reveals the avid quest for specificity is evident from: "However, we suspect that a *unique* arginine residue, in a fashion analogous to other protease inhibitors, forms the reactive site of the antithrombin–heparin cofactor".[158] This unwillingness to consider heparin–antithrombin as another example of "inverted binding" persists yet, even though many acidic heparin-binding proteins have one or more clearly positive domains.[159]

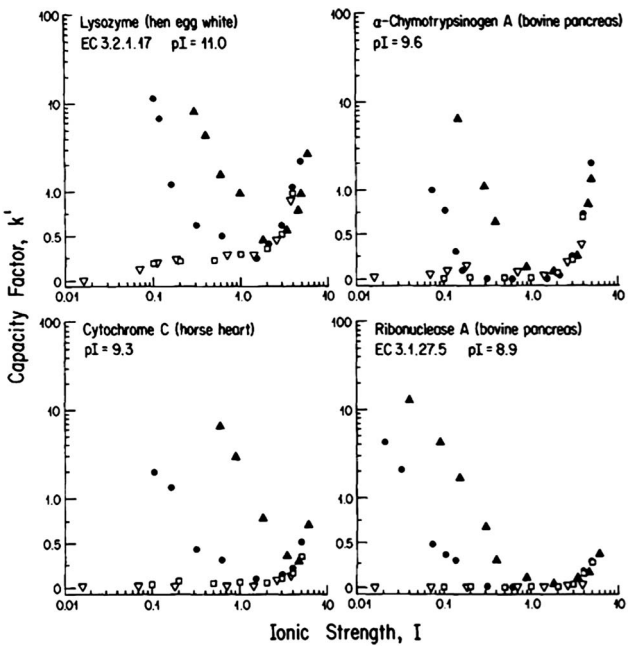

Fig. 4 Retention maps for 4 proteins on an anion exchange (positively charged) column. Capacity factors $k' > 1$ signify retention "on the wrong side of pI". Attributed in ref. 155 to negative charge patches.

Definitions of "charge patches" tend to be paradigm-specific. Doing computational modeling of protein ion exchange chromatography, Roush *et al.*[160] defined a charge domain as "a set of residues experimentally determined to be significantly involved in anion-exchange adsorption". On the other hand, from the perspective of molecular biology, a charge patch is likely defined as a set of conserved amino acids whose mutation blocks binding of some cognate macroions.[161] More precisely, Ren and Gorovsky using *in vitro* mutagenesis observed that regulation of a charge patch "need not be site specific…(as) the function of the modulation is to alter the charge of the domain in which it resides" (hence) "modulation of the charge at any one of a number of clustered sites can have the same effect".[162] "Charge patch" has been applied to non-PE–protein systems, for example, applying to liposome–DNA complexation, modeled as non-random adsorption of a polyelectrolyte producing polyion-rich and polyion-poor domains.[161] de Vries indeed wrote "there is no unique way of defining what a charge patch is", and – for the purposes of coarse-grained simulations of BLG binding to gum Arabic – defined it as a collection of protein charges of one sign closer to a central charge than to any single opposite charge;[163] this led to patches all smaller than 1 nm^2. A full-atom approach is more feasible when both participants are relatively rigid and well-defined, and Schreiber and co-workers have applied DelPhi calculations to obtain energies of interaction for protein cognate pairs, which were then compared to, *e.g.*, the measured ionic strength dependence of k_{on} and k_{off}.[164] These studies clearly define "charge domains" in the context of the particular protein–protein pair. Users of PyMol often fail to appreciate this, either because of a focus on qualitative visualization, or because of the assumption that the bound species is small compared to the protein, hence can be presumed to find its home close to the van der Waals surface. This is evidently not the case for the polyelectrolyte–protein system when ghost and hest may reverse the "normal" host–guest relationship.

Successive refinements of the protein patch in the protein–polyelectrolyte context have been sought by the senior author over the last 20 years. Measuring the pH at incipient complex formation, Park *et al.* found asymmetric behavior for different proteins, some exhibiting "wrong-side" binding with polycations, and some with polyanions, depending on charge anisotropy.[165] Based on earlier studies of binding to isotropic anionic micelles by the similar PEs, Park *et al.* suggested that the set of contiguous polymer segments that bind cooperatively would constrain the size of the "patch" to *ca.* 100 Å^2. If the length of the polymer is kept constant, binding affinity depends on polymer charge density, as seen by Mattison *et al.*[166] who suggested that the "charge patch" is an "array of charges on the protein surface which are complementary to the distribution of charges on the polyelectrolyte binding segment". The definition was further refined by Grymonpré *et al.*, who obtained DelPhi images of BSA at 5 different pairs of pH and I, all corresponding

to conditions of incipient hyaluronate binding.[167] A single positive protein domain (Fig. 5) was invariant with respect to the entire pH_c,*I* set, but changed appropriately with divergence from the pH,*I* regime of incipient coacervation. Finally, the five HA charges that could reasonably occupy the binding domain multiplied by the mean protein potential in their vicinity (*ca.* 0.1 kT/e), yielded a binding energy close to kT, thus providing three criteria for identification of the charge patch. This model however lacks an important component: repulsion, when a polyelectrolyte binds *via* a "charge patch" to a protein of like net charge. Conclusive evidence for this was found in the non-monotonic ionic strength dependence of binding affinity for binding "on the wrong side" for a variety of natural and semi-biotic protein–polyelectrolyte pairs.[168] All pairs showed a maximum in binding energy at an ionic strength at which the Debye length κ^{-1} was equal to the protein radius, a similar result obtained (even) for the "specific" binding of heparin to antithrombin III.[135] Thus the polyelectrolyte-binding domain of the protein can be defined by repulsions as well as attraction. Perhaps for this reason, the most dramatic "wrong-sided" binding of BSA is found at low salt concentrations (10 mM) with heparin, commencing at a critical pH more than two pH units above p*I*. With manifold variability of sulfation sequences, heparin can offer a particular sequence whose binding to the protein's positive domain is accomplished with minimal repulsion.

For protein adsorption in PE brushes, an alternate explanation "charge regulation" was proposed[169] and then vigorously extended to soluble complexes[170,171] (see also Section 4.2). This term refers to the ability of a PE to alter the effective pKs of amino acids. Therefore, Wen and Dubin[172] titrated BSA in the presence of an excess strong polycation, and found at pH 7 and low salt concentrations a shift in the expected direction of −4 charges (out of ∼60 titratable amino acids), but negligible effects at pH < 6, *i.e.* polycation-binding primarily shifted carboxylate p*K*s. On the other hand, Jonsson and co-workers[170,171] argued that "charge regulation" is the dominant effect for all protein–PE interactions. De Voss *et al.*[173] applied the self-consistent field approach, modeling the protein as a cylinder covered with weak acidic and basic charges immersed in an annealed (weak acid) brush, and concluded that charge regulation and patchiness have similar and additive effects of the same magnitude. Charge regulation alone however cannot explain the non-monotonic salt effects from conjoint attraction and repulsion,[168] or the fact that polycations are selective for proteins with a negative domain (*e.g.* separating the *less* acidic BLG from BSA (p*I*s 5.2 and 4.9)),[174] or that the strong polyanion PAMPS binds BSA (positive domain) at pH 6.9 (2.0 pH units above p*I*), but does not bind BLG (negative patch) until the pH is less than 6.2 (1.0 pH units above p*I*), or that modification of BLG by removal of 2 anionic residues in its negative patch lowers the pH required for polycation binding by 0.3 pH units.

To summarize, the "charge patch" is a consequence of intrinsic protein charge anisotropy, but is not defined until the species binding to it is. The principal issue is charge complementarity of the protein and polyelectrolyte which comprises both attraction and repulsion, the balance between them tuned by the Debye length. While the flexibility of the accessible protein units may be debatable, that of the polyelectrolyte partner (DNA excepted) is incontrovertible. Thus the polyelectrolyte has access to a vast array of local configurations within the relevant potential field of the protein, arrangements further multiplied by intra-chain heterogeneity either structural or in the case of annealed PEs induced. Recognition of the dynamic nature of the bound state reveals the necessity of dynamic simulations and visualization methods that reflect relevant potential surfaces.

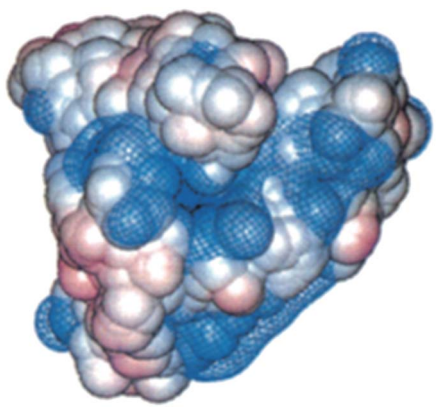

Fig. 5 Identification of the HA-binding site on BSA at pH 4.70, 0.15 M NaCl (upper region). The blue contour 5 Å from the vdW surface is the +0.05 kT per e potential.[167]

3.2 Soluble protein–PE complexes

Soluble protein–PE complexes can be examined from several points of view. From the colloid perspective, their coexistence with a separate phase *e.g.* coacervate could be represented by phase diagrams. From the polymer perspective, the complex might be described as a type of macromolecule with measurable dimensions and persistence length; in some circumstances this complex appears to be free-draining. Biophysical methodology and concepts of multiple binding equilibria should describe its relationship to free protein. Simulations proceed from the reductionist goal of seeking clearly defined interaction potentials. From the theoretical perspective, complexes exhibit critical formation conditions, akin to the theoretical results for polyelectrolytes and colloidal surfaces,[175–177] resulting from entrapment of *ca.* 5 neighboring polyion charges within a potential domain of about 5–7 mV.[178,179] Such cooperative binding is significantly complicated by protein charge anisotropy. All these approaches confront conceptual and practical limitations. Viewing the complex as a colloid particle ignores its dynamic nature and susceptibility to disproportionation (altering the distribution of proteins among polymer chains to promote aggregation or phase separation) and polarization (intrapolymer rearrangement of proteins). Dense and dilute phases may indeed co-exist but they do not differ merely in solute concentration. Invocation of polymer models is similarly challenged by the difficulty of defining the solvent and solute. Binding equilibria raise the conundrum of viewing the protein

as a ligand, while at the sub-nm scale, it acts as the substrate to which some sequences of contiguous PE residues bind cooperatively. Simulations confront the computational cost of full-atom descriptions, with the result that protein charge anisotropy is at best crudely represented, while for the polymer, the use of whole-chain persistence lengths with bead-spring models leads, in the absence of solvation, to overestimates of chain flexibility allowing PEs to wrap around proteins (DNA–chromatin notwithstanding).

Protein–polyelectrolyte soluble complexes are amenable to numerous characterization techniques many of which have already been treated in this review. These include circular dichroism, fluorescence anisotropy, capillary electrophoresis, viscometry, size exclusion chromatography, and all forms of scattering. Soluble complexes are equilibrium states, hence reversible with respect to stoichiometry, pH (most conveniently) and ionic strength (least conveniently). PEs can bind proteins quite efficiently, and the size of the protein-binding site on the polymer can be similar to the protein diameter.[180] Since PE can typically bind "on the wrong side of p*I*", charge reversal ($Z_T = Z_P + nZ_{pr} = 0$) can then occur as a function of pH, ionic strength and protein:PE stoichiometry, the first variable affecting both Z_{pr} and n, the others n alone. $Z_T = 0$ usually corresponds to the formation of soluble (or insoluble) aggregates. It should be noted that Z_T represents complex stoichiometry, while "[+]/[−]" usually, but sometimes ambiguously, signifies bulk stoichiometry. Disproportionation might play a role in phase separation above and below $Z_T = 0$,[180] an effect difficult to separate from system (particularly polyelectrolyte) heterogeneity. Evidence for perturbation of protein structure or function (see Section 5.1) is minimal. In fact, PEs appear to stabilize the native state thus inhibiting mechanisms of protein aggregation.

While intra-polymer and inter-polymer (aggregate) complexes have been detected, the former evidently the precursor, it is not clear whether the aggregates are intermediates between soluble complexes and phase separation. Direct evidence for disproportionation in coacervation is rare: transfer of proteins facilitating the formation of charge-neutral and hence coacervating complexes has not been established. A continuing problem in establishing boundaries between soluble complexes and either soluble aggregates or separate phases is system heterogeneity, either arising from component polydispersity or non-equilibrium mixing. The former is typical of heterogeneous components (*e.g.* whey protein), and the latter occurs when mixing sets up large concentration gradients, *i.e.* spatial variation in stoichiometry. If either leads to formation of non-fluid phases, the system becomes macroscopically heterogeneous and difficult to characterize.

3.3 Multilayers

Layer-by-layer (LbL) adsorption allows for the modulation of the surface composition and overall properties of polyelectrolyte multilayers (PEMs), and their subsequent interactions with (or alternatively incorporation of) proteins. The resultant protein loading capacity and protein function can be affected by the choice of PEs, in particular strong PEs as defined by permanent charges *vs.* weak PEs, with titratable functional groups. Since proteins can be associated with LbLs without loss of structure or loss of multimeric state (see below), LbL methods can be invaluable for protein immobilization, making them suitable for a wide range of applications.

3.3.1 Modulation of physical properties of multilayers by incorporation of proteins. PEMs can be generated with a wide range of physical properties and morphologies so that proteins can be immobilized (either incorporated within PEMs, or deposited on their surfaces) with different microstructural arrangements and to varying extents.[181] For example, Kreft *et al.* reported that peroxidase and glucose oxidase can be sequestered into separate compartments within "shell in shell" PEMs.[100] Bernsmann *et al.* reported that LbL films made of the bio-derived PE poly-dopamine were able to bind the 3 model proteins lysozyme, myoglobin, and α-lactalbumin due to a combination of covalent binding and attractive electrostatic effects.[182] Laos *et al.* reported that proteins were spactially separated from one another when adsorbed to a PEM.[62] Multilayers formed from the oppositely charged PE/protein pair hyaluronic acid (HA)/myoglobin, contain the most protein at pH < p*I*; however, a substantial amount of protein was incorporated into these PEMs above p*I* which suggests local interactions between HA and oppositely charged regions of the otherwise negative protein surface.[71]

3.3.2 Effect of pH. PEMs comprised of PEs with titratable functional groups are sensitive to pH which then controls PE effective charge density, and thus PE–PE interactions.[181] Kozlovskaya *et al.* found that solution conditions control swelling and layer thickness for poly(methacrylic acid) (PMAA) films templated on neutral polymers (poly(*N*-vinylpyrrolidone), PVPON).[183] Dai *et al.* reported that high protein incorporation into LbL assemblies of poly(acrylic acid) (PAA) was attained at a certain pH.[184] These PAA–protein layers bind to positively charged lysozyme at pH 7.4 (pH < p*I*) more strongly than to negatively charged BSA (pH > p*I*).[184] When both components are weak PEs, protein binding is observed in a narrow pH range for chitosan/alginate films, as shown by Yuan *et al.*[89] This narrowing of the complexation pH range results in target protein (IgG) binding maxima at pH 3.[89] Since IgG should be very positive at this pH, the multilayer itself must remain negatively charged either locally or overall, behavior that might be explained by charge regulation (see also Sections 3.1 and 4.2).[89] The conformation of poly(ethyleneimine)/poly(acrylic acid) (PEI/PAA) multilayers is very sensitive to pH which can be used to promote selective adsorption of one protein to the PEM surface.[139] On the other hand, Zhou *et al.* claimed that pH had little effect on protein binding of PEMs containing amine functional groups even though such PEMs are highly sensitive to ionic strength. Such films are also capable of binding proteins even below protein p*I*.[185] A 2006 review by Sukhishvili *et al.*[186] concludes that pH is an important variable in controlling the physical properties of these complexes since deposition is itself a result of the phase behavior of PE complexes in solution.

3.3.3 Effect of ionic strength. Ionic strength directly controls the interactions of proteins and PEMs similarly to the effects on interactions between soluble PEs and proteins. The swelling of PMAA–PVPON films is controlled not just by pH, but

also salt.[183] Hemoglobin and PSS were reported to form thicker multilayers at high *I*.[187] In contrast, proteins are effectively released from confinement within their multilayers with PMAA in 0.6 M NaCl due to the significant loss of attractive forces.[183] High *I* has also been suggested to decrease the overall protein selectivity of multilayers. Ionic strength also influences the presentation of protein "charge patches" to PEMs.[139]

3.3.4 Effect of temperature. Temperature controls the configuration of the flexible polymers within PEMs. However, it is not often selected as an experimental variable.[89,100,188–190] Multilayers comprised of cationic block copolymers and weak polyacids show reversible temperature sensitive swelling.[191] Temperature effects can result from shifts in polymer configuration (an entropic effect) or from shifts in the acid base equilibria that control the dissociation and subsequent charging of weak PEs.

3.3.5 Preservation of protein structure, function, and multimeric state. For a given protein–PEM system, protein native structure or function can be preserved by controlling the strength of electrostatic interactions. The strength of the electrostatic interactions within multilayers that incorporate proteins is usually controlled by pH, protein net charge and charge anisotropy. PSS/hemoglobin films are able to bind catalase on their surface without loss of function, as shown by preservation of enzymatic activity.[187] "Shell in shell" PEM capsules (Fig. 6) are permeable to small molecule substrates, and the enzymes contained within are still active.[100] Recombinant human bone morphogenetic protein 2 (rhBMP-2) can be trapped within PEMs formed from LbL assembly of poly-L-lysine (PLL) and hyaluronic acid (HA) for up to 10 days without loss of activity, suggesting no perturbation of native protein structure during complexation with these biocompatible multilayers.[106] Similar results are seen for preservation of BSA structures within LbL assembled PLL/HA capsules.[101] Chitosan/alginate multilayers can also adsorb proteins, specifically monoclonal antibodies, without loss of antibody activity.[89] Multilayers assembled from either poly(ethylene imine) (PEI) or polyallylamine hydrochloride (PAH), with oppositely charged poly(styrene sulfonate) (PSS) are shown to bind cytochrome-c on their surfaces with no detectable loss of redox activity even though some alteration of protein structure was detected.[192]

3.3.6 Select biological applications of PEMs. Since multilayers are able to interact with proteins under a wide range of conditions, they can be useful as biomaterials. PEM modified surfaces can be used to bind proteins, cells,[190] and even small inorganic counterions such as phosphate.[193] Such layers have been used for adsorbing growth factors.[188] They can also prevent fouling of protein under conditions of storage.[189] Other applications include biosensing[88,194] signal transduction,[98] proteins delivery,[195] reconstitution of bacterial proteins,[80] and modulation of biological pathways in order to control programmed cell death.[90]

3.4 PE brushes

Polymer brushes may be defined as dense layers of linear chains attached by one end to a substrate, with mean spacing less than the polymer size,[196] *i.e.* when $4R_g^2$ is large compared to the substrate area per chain. Interest in polyelectrolyte brushes had been particularly strong in the polyelectrolyte physics community because the effects of brush density and salt on polyelectrolyte stretching and layer thickness proved to be a fertile ground for theory[197,198] (the general field has been covered in several reviews).[199] The *ca.* 100 papers published since 2005,[10] grew to over 300 in the next six years, and the citation level per paper increased from 4 to 7 citations per paper, despite the short elapsed time. While studies of proteins in PE brushes have accounted for 10–15% of these totals, the average of 10–15 citations per paper indicates growing interest in this area.

The observation of protein uptake on anionic brushes above the p*I* attracted efforts in simulations and theory, although as noted above, this behavior is by no means unique to brushes, or to abiotic systems for that matter. As thoughtfully summarized by de Vos *et al.*,[173] this observation led to two hypotheses: one based on protein charge anisotropy (the "protein positive domain (*within a negative protein*) gains more energy from interacting with the negative brush than the negative brush loses"[173] (italics ours)) and the other (so-called "charge regulation" see also Section 3.1) based on the ability of the protein to attain a net positive charge due to the potential field of an anionic brush, even when the bulk pH exceeds p*I*.[170,200] As described above, charge anisotropy alone (without p*K* shift) provides a unique quantitative explanation of why binding to polyanions in solution at pH > p*I* is accompanied by non-monotonic salt dependence.[168] Still, there are clearly multiple ways in which the system may adjust to optimize electrostatic interactions. Protein charges are somewhat labile, *e.g.* binding of BSA to the strong polycation PDADMAC produces a small shift towards lower pK_a for acidic residues.[168] However, these effects are asymmetric: proteins with a positive charge patch bind more effectively to polyanions, and *vice versa* for those with a negative patch;[166] there is no uniform (independent of charge anisotropy) upward shift in p*I* upon binding to polyanions. For weak (annealed) polyanions, those charges are also labile, so that polyacrylic acid, for example, binds to cationic micelles more strongly than would a strong (quenched) polyanion of equal linear charge density.[201] This is similar to the recent theoretical finding of disproportionation of charges in annealed brushes.[202] Conversely, a highly charged (*e.g.* basic) protein can promote chain deprotonation.[203] Monte Carlo simulations for chains with sequence variability indicate that the protein may be offered a large menu from which to choose maximum charge complementarity. Finally, chain flexibility (even in a brush) offers another route to optimize short-range attraction/long-range repulsion (SALR). Resolution among these manifold effects is a formidable task for simulations.

More than binding "on the wrong side" of p*I*, the response of brushes to salt and pH (for weak polyelectrolyte brushes) offers new ways to control protein uptake and release without perturbation of native state structure. It has been firmly established that enzymes retain activity in PE brushes, *e.g.* beta-galactosidase in a PSS brush,[204] or glucosidase on a PAA brush. Similarly, secondary structures are preserved on planar PE brushes for lysozyme, BSA, α-lactalbumin and insulin.[205] This

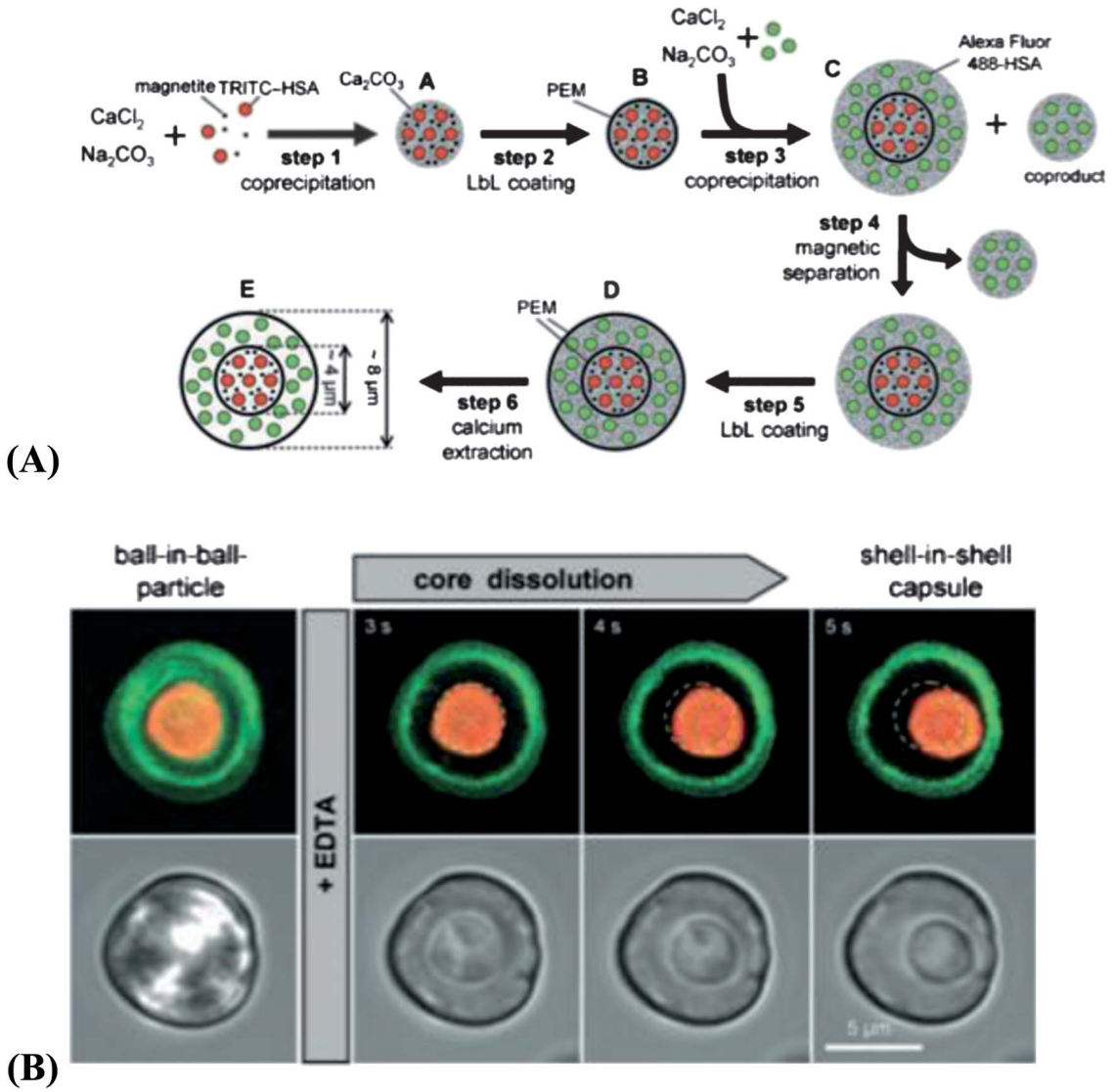

Fig. 6 LbL synthesis results in formation of "shell in shell" PE microcapsules that can sequester protein.[100] (A) Outlines a typical synthetic route. (B) Confocal microscopy showing pH induced dissolution of microcapsules resulting in controlled release of fluorescently tagged BSA.

has been attributed to the weak (transient) binding of the protein.[173] On the other hand, ribonuclease absorbed in a similar brush displays a decrease by 10 °C in the unfolding temperature.[206] Protein instability seems most likely to occur for hydrophobic proteins on similarly amphiphilic polymers, *e.g.* the polystyrene brush core.[207]

The mechanisms and energetics of protein adsorption comprise not only enthalpic contributions (hydrophobic, coulombic, hydrogen bonding) but also the entropy of release of counterions and water. It has been suggested that the driving force for adsorption is the displacement of counterions by protein domains of like charge.[208] The accumulation of excess counterions within the brush has been proposed to provide local neutrality, *i.e.* equal in number to the PE charges.[209] Protein charge anisotropy can allow for asymmetric interactions with the polyelectrolyte brush, even for net neutral proteins.[210] The role of "charge patches" in promoting counterion release has been emphasized in regard to the predominance of the entropy of binding for BLG on PSS brushes detected by ITC.[60] Such an entropy gain should vanish when the external (bulk) salt concentration is no longer lower than the brush (internal) salt concentration, but this effect can be concurrent with internal screening of protein–brush interactions, and with steric repulsion due to brush collapse. Furthermore, in this case (the "salted regime") the counterion osmotic pressure shrinks along with the brush, proteins are repelled by steric interaction, and protein adsorption may resemble that seen for hydrophobic surfaces.[211] Contrariwise, in the unsalted or "osmotic regime" brushes are comprised of stretched chains with high local counterion concentrations, and chains may rearrange.

While spherical brushes can be studied by many solution techniques, planar brushes allow for the use of other methods, such as surface plasmon resonance. Kusumo *et al.*[65] measured the uptake of BSA on PDAEMA brushes on gold and found remarkably high levels of protein adsorption, linear with polycation surface concentration, indicating that individual chains

are "decorated" with protein, each BSA occupying about 40 nm of chain contour length. They found that the amount of BSA adsorbed increased with grafting density, similar to the result of de Vos *et al.*,[200] but only for low MW. de Vos also observed a chain length effect: more BSA was adsorbed when PAA MW increased from 9 to 19 kDa. It was proposed that binding might involve protein negative charge patches, even at pH 4. These authors did not consider p*K* shifts and alteration of charge sequences in this "annealed" polycation. Stamm *et al.* studied the adsorption of BSA on 5 nm grafted PAA layers (so-called Guiselin brush). Using a wide range of techniques including QCMD and ellipsometry they showed a coupling of protein and small ion adsorption, and conjoint effects of brush swelling and protein release.[85] Zimmermann *et al.*[212] were able to use streaming potential and reflectometry to examine the uptake of fibronectin (p$I \sim 5$) on a grafted PGA brush which itself was subjected to a helix-coil transition (pH switching)[212] leading to transition in brush dimensions. The mobility of ions within the brush was only 15% of the bulk value. They concluded that protein uptake was electrostatic in nature, and speculated about "charge orientation in the interfacial layer". PAA on a gold surface also provides a pH-switchable brush that can be studied by electrochemical impedance spectroscopy.[213] Electron transfer between the electrode and protein is facilitated by the polyanion brush, although interactions with it slow down the diffusion of cytochrome C. When such interactions are diminished at lower pH the protein is released. With novel synthetic procedures,[184] PAA brushes on gold can be >100 nm thick and these can adsorb lysozyme at pH 7.2, at a level equivalent to 80 monolayers. However, BSA and myoglobin would not adsorb without derivatizing the brush to introduce metal-ion affinity. The fact that lysozyme binding increases with brush thickness suggests that lysozyme resides everywhere in the brush.[214] A similar conclusion was reached by Kusumo *et al.*[65] based on the finding of a constant protein (BSA): brush repeat unit (DMAEMA), regardless of grafting density.

An essentially distinct literature focuses on elimination of protein adsorption, for biomaterials and drug delivery devices, or for antifouling in biosensors and marine coatings. Zwitterionic polymers are of special interest. Their protein resistance has been thought to arise from hydration layers.[215,216] Even papers that focused on protein adsorption are cited primarily from this perspective. An additional application for polyanionic brushes is "biomimetic" in the sense that heparin-like chains might resemble brush-like glycosaminoglycan structures in ECM or cell surface proteoglycans, which clearly resist non-specific protein adsorption.[217] Analogies between brushes and neurofilaments have been pointed out.[218] A most intriguing observation coming from ATR-FTIR studies[205] is the failure of insulin in brushes to form fibrils under conditions of very low pH and high temperature at which fibrilogenesis usually occurs.

3.5 Gels, hydrogels

A polyelectrolyte hydrogel is a charged polymer network surrounded by counterions. Crosslinked polyelectrolyte hydrogels undergo network swelling and deswelling due to their capacity to absorb large amounts of water. This property can be determined by the gelation process[219] and facilitates the uptake and release of proteins[220,221] *via* environmental triggers such as pH, temperature, and ionic strength.[222] Several types of hydrogels will be reviewed in the section.

3.5.1 Stimuli-responsive hydrogels. Themoresponsive hydrogels are receiving more attention recently in biomedical fields as the protein loading and release process does not require external additives. Thermosentitivity of such hydrogels relies on the reversible thermal phase transition of polymers, characterized by lower or upper critical solution temperatures (LCST or UCST).[223] Lü *et al.*[224] reported a thermoresponsive hydrogel prepared from poly(*N*-vinyl-pyrrolidone) (PVP) and carboxymethyl-cellulose (CMC). As shown below in Fig. 7, at temperatures under the volume phase transition temperature (VPTT), PVP/water and CMC/water hydrogen bonding dominates resulting in an enthalpically driven swelling process. At $T >$ VPTT, hydrophobic interactions between PVP and CMC dominate leading to the release of water molecules, thus deswelling must be an entropically driven process.

pH constitutes a second variable in the design of responsive physical gels for biomedical applications. These hydrogels are often prepared from pH-sensitive polyelectrolytes such as weak polyacids or polybases whose ionization states depend on the pK_a values of the relevant acidic or basic groups. Liu *et al.* studied carboxymethyl chitosan hydrogel beads crosslinked by Ca^{2+}.[225] The hydrogel was observed to swell at high pH due to the formation of insoluble $Ca(OH)_2$. This pH dependence of swelling and deswelling was then used to load and release BSA (a model for drug delivery). Li *et al.*[226] studied the effect of lysozyme binding affinity on its uptake by negatively charged oxidized potato starch polymer hydrogels under different conditions of pH and ionic strength, and found binding affinity and capacity highest at pH 5 and low salt concentrations. Lysozyme binding affinity and binding capacity are highest at pH 5 and low salt conditions. Shi *et al.*[227] reported a composite hydrogel prepared from *N*-[(2-hydroxy-3-trimethylammonium) propyl] chitosan chloride (HTCC) with modification of glycidyltrimethyl ammoniumchloride (GTMAC). This hydrogel showed both pH and thermal response and was used for entrapment and release of insulin with full retention of bioactivity. Polymeric hydrogel capsules have recently been developed as next generation protein carriers.[228] Zelikin *et al.*[229]

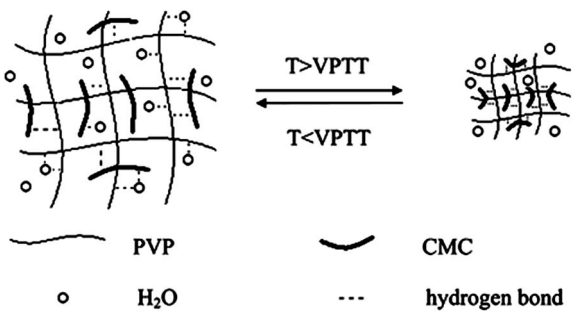

Fig. 7 Schematic illustration of PVP–CMC hydrogel structure before and after phase separation.[224]

showed sequential deposition of thiolated poly(methacrylic acid) (PMASH), poly(vinylpyrrolidone) (PVPON) and disulfide crosslinking onto silica particles (Fig. 8). Removal of the silica particles generates a hollow biodegradable hydrogel capsule applicable for protein delivery. This capsule undergoes swelling as pH is changed due to the disruption of hydrogen bonding between PMA_{SH} and PVPON. In addition, the cleavage of disulfide bonds in the reducing environment present in the cell should degrade the capsule.

3.5.2 Other stimuli-responsive hydrogels. Besides heat and pH, other components such as inorganic ions were recently shown by Oh *et al.*[230] to bind to negatively charged sites of the cross-linked poly(acrylic acid) (PAA) and poly-(ethyleneoxide) (PEO) hydrogel to release BSA.

3.5.3 Protein diffusion in hydrogels. The mobility of proteins in a hydrogel is especially important for protein encapsulation. Li found that the diffusion coefficient of free lysozyme is one order of magnitude lower than that in bulk solution due to the electrostatic binding of protein to the gel and obstruction by the gel network.[103] Li *et al.*[108] also investigated lysozyme diffusion in oxidized starch polymer hydrogels. Several bound protein fractions of different mobilities were found, indicating different binding affinities of lysozyme to hydrogels. Such different binding affinities are determined by the limited number of binding sites to which proteins are bound. High ionic strength and high pH lead to diminution of electrostatic interaction leading to larger populations of more mobile protein. It was also found that protein release kinetics were directly related to the mechanical and structural properties of the hydrogel.

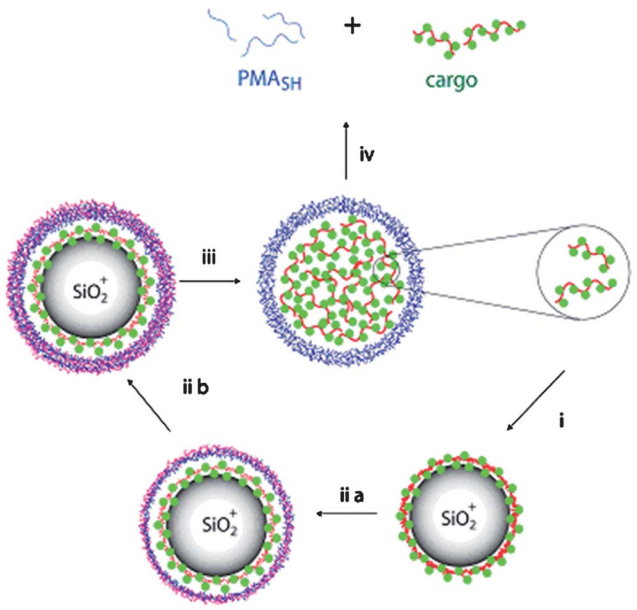

Fig. 8 For loading, cargo molecules are immobilized onto the surface of the template particles (in this case positively charged silica, SiO_2^+, step (i)). Sequential deposition of polymers (ii), removal of template and release of PVP (iii) result in single component PMA hydrogel capsules with cargo molecules occupying the central void of the capsule.[229]

Proteins usually diffuse most readily in the gel during the initial periods of protein loading and release. Hence, additional strategies have been applied to control the release process. As shown by Kim *et al.*,[231] coating of flexible alginate microgels with the stiffer biopolymer, chitosan, leads to lower protein release rates, showing the coupling of mechanical properties with protein release profiles in alginate microcapsules. Park *et al.* reported on thermosensitive poly(organophosphazene) hydrogels as an injectable gel–depot system for protein delivery. A layer of PE complex was then introduced to control the release process.[151] Li *et al.*[109] also studied the stabilization of a negative hydrogel by a poly(L-lysine)–poly(L-glutamic acid) complex layer, leading to a much slower release rate of lysozyme.

3.6 Coacervates

Coacervation, discovered as described in the elegant studies of Bungenberg de Jong in the 1920s,[232] was directed towards microencapsulation between the 1960s and 1980s. The field reawoke in the early 1990s based on the interest of colloid and polymer scientists in the fundamentals of coacervate formation. Incorporation of sophisticated characterization techniques such as DLS, SANS, rheology, FRAP, PFG-NMR, cryo-TEM, and confocal microscopy, has helped to elevate the field above the radar. A Web of Science search for "complex coacervation" reveals 164 papers before 2000, jumping to 476 after 2000. Despite this newly gained recognition, there is confusion about the difference between coacervates and other electrostatic association-based states such as flocculates or films established through layer-by-layer assembly of polyelectrolytes with proteins. Here we will present findings on the topic since our 2005 review[10] and will also note some new insights from other recent reviews.[11,34,38,233]

3.6.1 Definition and differences from other electrostatically driven phase separations. Protein–polyelectrolyte coacervation is a liquid–liquid phase separation driven by the electrostatic interactions between oppositely charged macroions and by the entropy gain attained through the release of counterions. The turbid phase obtained by mixing of proteins with polyelectrolytes contains spherical droplets of a few micrometers.[11,234,235] These droplets coalesce to separate into two liquid phases either by centrifugation, or gradual settling in a few days. Mixtures that stay turbid for more than three weeks are considered as "incomplete coacervates".[38,236] If the phase separation is complete, the upper phase is a dilute equilibrium liquid ("supernatant") while the lower one is the coacervate. Depending on the strength of interactions, the coacervate may be a gel-like fluid or viscous liquid, rich in macromolecules (10–20% by wt) and water (80–90%). In the absence of severe heterogeneities, the coacervate phase is optically clear.

It is relatively easy to differentiate coacervates from precipitates but not so easy with flocculates or other colloidal fluids, as shown in Fig. 9. Cousin *et al.*[38] suggested a clear distinction between these different terms based on macroscopic observations and SANS measurements: precipitation is a solid–liquid separation, where the dense phase has crystalline features. Flocculates or flocs are also formed through solid–liquid phase

separation but the less dense phase, floc, stays suspended in the solution for a longer time. Precipitation usually follows when macromolecular charge densities are high enough to facilitate loss of counterions and concomitant desolvation. It has also been suggested that chain flexibility contributes to the preservation of water in the vicinity of macromolecules, thereby promoting coacervation, with the more rigid polyelectrolyte chains leading to precipitates (ref. 11 and references therein). Readers are referred to the excellent review by Boué and coworkers[38] for differences in the mesoscale structure of coacervates *versus* precipitates. Compared to polyelectrolyte hydrogels, which require more than 5 weight% polymers in order to gel, coacervates can be formed from polymers and protein solutions at concentrations as low as 0.1 wt%. Compared to the layer-by-layer self-assembly of polyelectrolytes with proteins, important rearrangements occur in the coacervation process guided by a combination of short-range Coulombic attractions with long-range Columbic repulsions and counterion release, so that coacervates can have rheological properties and mesophase structures unlike polyelectrolyte–protein multilayers. These differences will be discussed in more detail below.

3.6.2 Factors affecting the onset of coacervation. Factors affecting coacervation are numerous: pH, *I*, polymer stiffness, PE charge density, protein charge anisotropy, protein–PE charge ratio, temperature, polymer chain length, and protein MW. In this section, we will discuss the most important parameters.

3.6.2.1 Soluble complexes and charge neutrality. Formation of soluble complexes precedes polyelectrolyte–protein coacervation. As mentioned in the previous sections, a soluble complex includes a polyelectrolyte and multiple proteins electrostatically coupled *via* binding energies in excess of thermal energy. Here, the proteins involved in this complexation might have either an opposite net charge or an opposite "charge patch". If the net charge of soluble complexes is too large, long-range repulsions among them provide stability without further structural rearrangement. Upon adjustment of pH or ionic strength, the net charge might be close enough to zero so that inter-complex repulsion is not sustained.[237] Soluble complexes then proceed, usually with higher order association, to coacervates. Experimentally, the onset of coacervation for protein–polyelectrolyte coacervates is determined by the pH (pH_φ) where turbidity shows a sharp increase within ± 0.1 units in the absence of system heterogeneity. At pH_φ, the "zeta potential" of the system is zero or close to zero,[238,239] which correlates with charge neutrality of aggregates.

3.6.2.2 Ionic strength. Charge screening lessens the strength of electrostatic interactions, therefore requiring a higher or a lower pH_φ for polycation–protein and polyanion–protein systems, respectively. More interesting is the suppression of coacervation at very low or high salt concentrations for some protein–polyelectrolyte systems. BSA–PDADMAC, BLG–PDADMAC, and β-lactoglobulin–pectin coacervates all show non-monotonic dependence of pH_φ on ionic strength.[174,240] These effects arise from the influence of pH and *I* on the net complex charge $Z_T = Z_P + nZ_{pr}$. Since Z_T must be close to zero for coacervation, the effect of *I* on *n*, and the effect of pH on both *n* and Z_{pr} account for the conjoint effect of these two variables on the point of coacervation. When more salt is added at low *I*, PE–protein interactions can be screened thus decreasing *n*, while inter-protein repulsions are also diminished, increasing *n*. These complex effects result in the non-monotonic behavior such that addition of salt can result in coacervation followed by return to the one-phase state. At the high *I* regime, the entropy gain from counterion release will be less since the concentration of counterions condensed within the coacervate will be approximately equal to the concentration of small ions in the continuous phase.[235] Chain stiffness and degree of protonation for weak polyelectrolytes are additional parameters affecting the ionic strength dependence of pH_φ. Coacervates of BSA with chitosan, similar in charge density but less flexible than PDADMAC show lower values for pH_φ at low *I*.[21] Coacervation is favored for chitosan due to (1) an increase in the configurational entropy upon coacervation, and (2) the avoidance of charge repulsion by mobility of charge domains on chitosan. On the other hand, pH_φ is not dependent on *I* for coacervates of gelatin B and agar.[237] Complicated chemical compositions of these two biomacromolecules make it difficult to resolve contributions to the onset of coacervation.

3.6.2.3 Protein–PE stoichiometry. Stoichiometry can be represented in terms of macroion charge or macromolecule mass. Charge ratios tend to refer to the stoichiometry of the complex, with weight ratios usually signifying bulk ratios, the two being equivalent only for high-affinity binding together with variable microstoichiometry. To the extent that bulk stoichiometry controls microstoichiometry, coacervation can be suppressed at

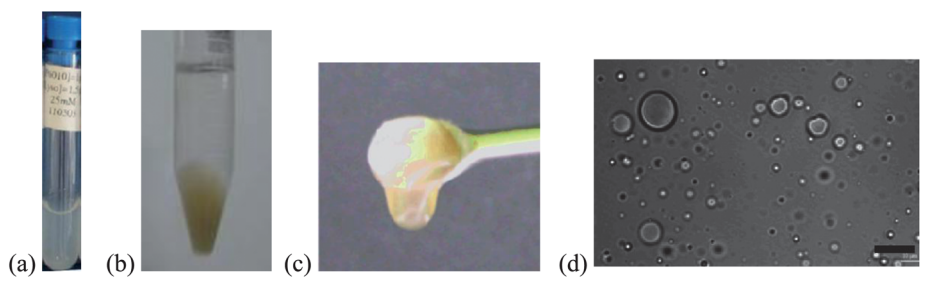

Fig. 9 (a) Incomplete ("pseudo-") coacervate of pectin and lysozyme.[38] (b) Coacervate (bottom) phase and dilute (top) phase of gum Arabic/chitosan. (c) Coacervates of hyaluronic acid – recombinant mussel foot protein-5 (mfp-5).[234] (d) Droplets observed within coacervate suspension of total acacia gum/β-lactoglobulin (BLG). Scale bar: 20 μm.[235]

very low and very high protein–polyelectrolyte weight ratios.[21] At an intermediate protein–polyelectrolyte ratio (r), pH_φ increases with r for the BLG–pectin system.[22] When there is more BLG in solution, more BLG binds, resulting in charge neutralization at a higher pH. Coacervation between positively charged protein and negatively charged synthetic polyanions is enhanced at the charge equivalence point,[241] *i.e.* $[-]/[+] = 1$. In addition, structural complementarity is crucial for coacervation. Highly asymmetric charge spacing favors soluble complexation over coacervation,[21] while highly similar charge spacing favors precipitation, as in polyelectrolyte–polyelectrolyte systems,[242] such as scrambled polysalts.

3.6.2.4 Polyelectrolyte charge density (local and global). Polyelectrolyte charge densities modulate the onset of coacervation. The dependence of pH_φ on I changed from a monotonic decrease for BLG with 30% carboxylated[22] pectin to non-monotonic behavior for 70% carboxylated pectin with blocky charge sequences (methyl ester distribution). The influence of local charge density on the onset of coacervation could be evaluated more directly by comparing pectins of similar charge density but different degrees of blockiness. At low I and for $r \leq 2$, coacervation occurs more readily for pectin with 11% blockiness *vs.* 1.7% blockiness. The lower pH_φ may be attributed to a higher local charge density.

3.6.2.5 Temperature. For reasons not fully understood, the effect of temperature on pH_φ appears to depend on the polyelectrolyte–protein pair. While PDADMAC–BSA coacervation[243] or its coacervate structure[152] showed no dependence on temperature, chitosan–BSA coacervates[33] went through structural changes at pH < 18 °C and pH > 27 °C. For pea protein isolate and gum Arabic, pH_φ increased with a decrease in temperature from 23 °C to 6 °C, which was attributed to contributions of hydrogen bonding between the biomacromolecules.[231]

3.6.3 Thermodynamics of coacervation. Relative contributions of enthalpy and entropy to the Gibbs free energy of mixing determine the dominant driving force for the self-assembly of coacervates, which requires $\Delta G_\varphi = \Delta H_\varphi - T\Delta S_\varphi < 0$. Recent studies analyzed ITC results with a model of two-stage structuring.[11,129,235] Exothermic peaks are observed during the initial steps of titration of BLG[235] with gum Arabic.[244] In the second step, the enthalpy change either becomes positive or goes to zero, thus indicating that $\Delta S > 0$. This entropy gain is mostly a result of release of counterions and water molecules from the neighborhood of the macromolecules.

3.6.4 Coacervation models and theories. In recent years, several models of coacervation self-assembly evolved. One depicts the coacervate as a transient physical network cross-linked electrostatically by several proteins at the junction points.[152,245] In a second model,[33,152] transiently charge-polarized regions are first formed within soluble complexes. This polarization might originate from "charge migration" within weak polyelectrolytes or concentration fluctuations.[246] These transiently charge-polarized regions drive association of complexes into soluble interpolymer complexes, followed by higher order association to form relatively dehydrated clusters with near-zero charge that coexist with soluble complexes. Cluster sizes are stabilized by short-range attractions and long-range repulsions both Coulombic in nature. SANS studies on the polystyrene–lysozyme system[37–132] suggest that the second model may be improved by considering excess charges in a shell around the cluster. Veis' new model[247] also accounts for the excess charge density or chain length: the chain with the excess charge always goes to the dilute phase. The structure of the aggregates in the coacervate phase may be random or symmetrical. Zhang and Shklovskii[180] considered "condensation" (coacervation) in the presence of excess charge. In the case of $[-]/[+] \neq 1$, polyelectrolytes might disproportionate in two possible ways: (a) inter-complex disproportionation, in which some oppositely charged polyelectrolytes condense as neutral macroscopic drops while others form charged complexes or stay free; (b) intra-complex disproportionation, in which migration of polyions within a complex occurs to form a neutral region with excess charge at an end. No model or theory developed this time takes into account the redistribution of counterions in coacervation, which are pointed out by experiments.[248]

3.6.5 Protein in coacervates. There are conflicting results in the literature about the maintenance of protein secondary structure in coacervates. Coacervation of β-lactoglobulin with acacia gum and alpha-gliadin with acacia gum, pea globulin with acacia gum reportedly led to changes either on the alpha-helical or beta-sheet structure.[249] On the other hand, Nickerson and his coworkers observed minimal change in pea protein structure in its coacervates with alginate.[250]

3.6.6 Mesophase structure. Spatial heterogeneity of proteins and polyelectrolytes has recently been uncovered through scattering, rheology, cryoTEM, and PFG-NMR.[112,132,142–146] Depending on the charge state of proteins and polyelectrolytes, and the chain flexibility of the latter, the coacervate phase might (a) have no spatial ordering, (b) have a random structure, or (c) have near-spherical or rod-like compact structures. Coacervates of gelatin B and agar showed inhomogeneity sizes of 2.4–4 nm with increasing salt concentration, while the correlation length of concentration fluctuations was around *ca.* 2 nm independent of I.[251] Coacervates of BSA with PDADMAC or chitosan had a random distribution of irregular and partially connected solid-like "clusters", which range from tens of nanometers to hundreds of nanometers (Fig. 10).[127] Coacervates of BSA with chitosan – less flexible than PDADMAC – form under weak electrostatic interaction conditions. DLS suggests chitosan domains to be less dense, while rheology and SANS suggest them to be more interconnected and to occupy a larger volume fraction.

Compact structures were found for coacervates formed at a low charge ratio with flexible polyelectrolyte-containing systems such as lysozyme and poly(sodium(sulfamate-carboxylate)-isoprene).[55] Nonstoichiometry at higher charge ratio is resolved by formation of a "hairy" shell structure around the neutral core. Stiff polyelectrolytes, on the other hand, tend to arrange in rod-like "aggregates", which enable them to attain charge neutrality at low protein charge, as observed in coacervates of hyaluronic acid and lysozyme[48] or chitosan and BSA.[33]

The size of the lactoferrin–casein aggregates increases "indefinitely and asymptotically" near charge neutrality.[252] Anema and de Kruif have proposed that the size of coacervate

aggregates is limited by the surface charge at charge fractions away from the charge equivalence point. This proposal agrees well with previous discussions on why coacervate aggregates and clusters do not fuse further to go through a subsequent microphase separation.[32]

3.6.7 Cognate coacervate systems

3.6.7.1 Natural underwater adhesives. New insights into complex coacervation come from the adhesive properties of sandcastle worms and caddisfly larvae. Sandcastle worms produce acidic (rich in phosphates) and basic (rich in amines) proteins, which are presumed to coacervate before secretion into seawater (Fig. 11). At the higher pH of seawater, the coacervate "glue" hardens into a solid. Caddisfly larvae secrete silk fibroin with alternating positive and negative patches on the same protein. Its coacervation resembles that of gelatin in as much as both involve amphoteric proteins.[253]

3.6.7.2 Role in elastin coacervation. Coacervation among "monomers" of tropoelastin, the precursor protein of elastin, is driven by hydrophobic interactions.[254] Particularly relevant to our review are studies indicating an enhancement in tropoelastin coacervation by cell-surface bound glycosaminoglycans. Addition of heparin sulfate or dermatan sulfate into tropoelastin solutions decreased the critical coacervation concentration of tropoelastin, possibly by reducing the repulsion between tropoelastins. It would be interesting to investigate whether dilute solutions of tropoelastins and GAGs form coacervates upon change in pH or *I*.

3.6.8 Applications

3.6.8.1 Microencapsulation. In the six years since our last review, microencapsulation of food ingredients continues to be the major application of coacervates.[255,256] A recent encapsulation method proposed as a stimuli-responsive drug delivery platform involves forming protein–PE coacervates within the water channels of amphiphilic cubic phases.[257] Coacervates formed between hydrophobically modified alginate and hydrophobically modified silk fibroin entrap the "model drug" (FITC–dextran).[257] Upon increase of pH, FITC–dextran was released through coacervate dissolution. Phase change materials (PCM) such as mixtures of *N*-alkanes are also microencapsulated by gum Arabic–gelatin or agar–Arabic gum coacervation to store thermal energy.[110]

3.6.8.2 Separation of proteins. Industrial purification of proteins conventionally involves costly and time-consuming processes such as liquid chromatography and membrane separation. These techniques are not efficient in achieving separation of proteins with isoelectric points differing by less than 0.5 pH units. Xu *et al.* separated genetic variants of BLG, BLG-A and BLG-B, which only differ by one amino acid; BLG-A contains aspartic acid in position 64 while BLG-B has glycine.[174] pH_{φ} for BLG-A and PDADMAC was slightly lower than that for BLG-B. Stronger electrostatic interactions between the relatively larger negative "charge patch" of BLG-A and PDADMAC lead to an increase in the BLG-A content in coacervates. *I* and pH control both selectivity and yield for selective coacervation of proteins with oppositely charged polyelectrolytes.

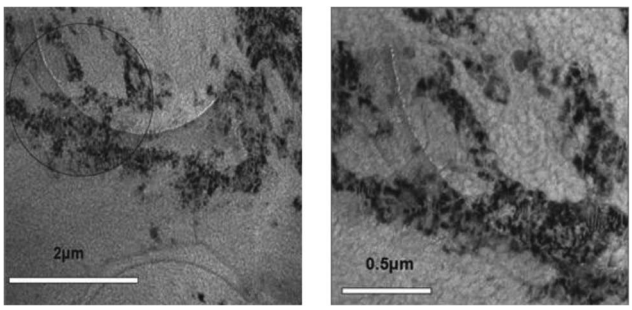

Fig. 10 Cryo-TEM images of BSA–PDADMAC coacervate at pH = 9.0, *I* = 0.05 M NaCl.[127]

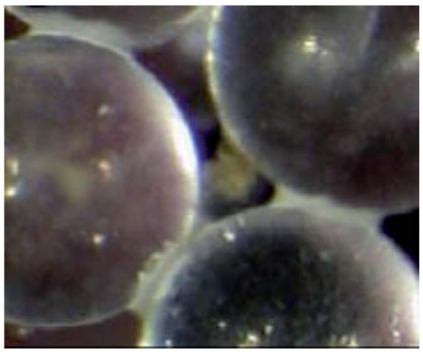

Fig. 11 Glue of the sandcastle worm sticks silica particles together.[253]

3.6.8.3 Biomimetic adhesives for wet surfaces. Oppositely charged protein and polyelectrolyte systems were inspired by the models of natural underwater adhesives (see above). In these systems, either the protein or the polyelectrolyte contains 3,4-dihydroxyphenyl-L-alanine (DOPA), the amino acid responsible for hardening of the fluid glue secreted by sandcastle worm, caddisfly larvae, and marine mussels. The adhesive strength of coacervates formed between recombinant mussel adhesive protein fp-5 and hyaluronic acid was 1.73 MPa on aluminum, 1.5 fold larger than recombinant fp-5 alone.[234] Thus, Stewart and coworkers prepared coacervates from poly(phospho-dopamine) and aminated gelatin to produce a bond strength of *ca.* 500 kPa in the presence of periodate.[258] The difference between the adhesive strengths might be a result of different strengths of interactions.

Studies of polyelectrolyte complexes, which can be prepared from numerous pairs of polyelectrolytes, predate studies on protein–polyelectrolyte complexes, but examinations of the ternary systems are a new direction. In the one case, the ternary complex is formed from a mixture of two like charged PEs and an oppositely charged protein. In this case the driving force is PE–protein interaction. Protein charge anisotropy can also allow a protein to interact with positive and negative PEs simultaneously. In the second case, complexes are formed from two oppositely charged PEs, which then interact with proteins.

3.7 Ternary complexes

Ternary mixtures of like charged trimethylchitosan and trimethylchitosan/PEG copolymers with insulin at pH 6.8 have been shown to result in stable spherical insulin-containing particles.[93] Additionally, beads coated with mixtures of

carboxymethyl chitosan and unmodified chitosan can form ternary complexes with BSA. Such complexation involves attractive interactions between PE and protein, but PE–PE repulsive interactions were not considered.[225] Swelling behavior of the resulting complexes was further studied at highly acidic conditions (pH < 2) and at physiological buffer conditions (pH 7.4). Surprisingly, maximum swelling was observed at pH 7.4,[225] despite the strongly positive protein charge at pH < 2 which should maximize repulsions between the cationic PE pair and the protein.[225]

3.7.1 Ternary systems comprised of two oppositely charged PEs. Complexes or nanoparticles formed from oppositely charged PEs can bind proteins. de Vasconcelos *et al.* showed that assembling nanoparticles from binary mixtures of polycation chitosan and poly(methacrylic acid) (PMAA) will result in the formation of negative PMAA coated particles.[111] Subsequent interactions with BSA first occur near p*I* where a positive protein domain interacts with the PMAA coating and a negative charge patch interacts with the positive chitosan core.[111] Hartig examined the effects of the MW and stoichiometry of the polymers comprising binary PE complexes.[259] The results suggest that the chain lengths and charge densities of the polycationic and polyanionic components must be closely matched to allow for the formation of soluble complexes that can persist and interact with proteins over a wide pH range.

3.7.2 Applications of ternary PECs. Ternary complexes formed from a wide range of biologically compatible PEs have many applications due in part to selective complexation and release of proteins by means of their complex swelling behavior. Beads formed from chitosan–alginate mixtures can be used to trap BSA at pH 6.8 (pH > p*I*) and release it only at acidic pH (pH < 2) where repulsive interactions dominate.[260] PECs formed from other oppositely charged bioderived PEs often provide biocompatible amphiphilic materials. Their properties include cell adhesion,[261] and their applications include biocompatible delivery systems,[262] and biodegradable implants.[263] Other applications include formulations of colloidally stable dispersions of pharmaceutical proteins such as insulin,[112] or construction of tissue scaffolds.[264] These systems immobilize proteins with minimal perturbation as demonstrated for alginate–chitosan–insulin particles.[140]

3.8 Cognate–PE systems

Protein–PE systems can be categorized as abiotic (synthetic polymers), natural (bioderived polymers with non-cognate proteins), or cognate (PE and protein co-evolved). The differences between the first two are differences of terminology, but the difference between them and the third arises more from their respective paradigms and models, than from fundamental differences among interactions.

Since the helicity of DNA renders it so unique, we focus here on glycosaminoglycan (GAG)–protein interactions. GAGs are highly sulfated linear polysaccharides found on cell surfaces, in the extracellular matrix (ECM) and in mast cell granules. They bind to a large array of proteins including matrix components, enzymes, enzyme inhibitors, growth factor families and receptors, and cytokines and chemokines, to regulate physiological processes. The main challenge is the highly heterogeneous GAG structure due to non-template driven biosynthesis *via* post-translational modifications. In many studies related to GAG–protein interactions, GAG structure is improperly depicted as rigid, and the dynamic nature of these highly charged polysaccharides in solution has not been given enough attention.[265]

GAGs exhibit polyelectrolyte behavior in solution, as unambiguous observation by Jacques, subsequently ignored.[266] Key polyelectrolyte parameters are its high linear charge density, salt dependent chain stiffness, and characteristic dependences of chain dimensions on MW and ionic strength. The exceptionally high linear charge density arises from extensive post-translational sulfation. Through a variety of physicochemical techniques, Pavlov *et al.* clearly characterized heparin as a semi-flexible, worm-like PE chain.[267] Bertini *et al.* employed high performance-size exclusion chromatography (HP-SEC) with a triple array detector to calculate the molecular weight and molecular weight distributions of full-length heparin, heparin fractions and dermatan sulfate. Consistent with the worm-like chain model, they found intrinsic viscosity $[\eta]$ to scale with $MW^{0.84}$. Different GAGs exhibited different MW-dependence of $[\eta]$ and of the radius of gyration which could be related to structural and configurational differences.[268] Guo *et al.* showed that accurate measurement of MWs of heparin by size exclusion chromatography required salts (1 M) to screen electrostatic interactions with the column packing.[269] An essential feature of nearly all polyelectrolytes in solution is flexibility and stochastic chain dimensions. The dynamic nature of GAGs was considered by Lander who emphasized their contribution to the kinetics of protein binding rather than thermodynamics.[270] He proposed that GAGs act catalytically on the cell surface to capture growth factors and their receptors. In blood coagulation, heparin basically increases the rate of antithrombin–thrombin or Factor Xa interaction. Accordingly, the interaction can be considered in two steps: encounter and reaction. The first is driven by the physics of diffusion for the binding of AT and the coagulation protease on the same heparin chain (the GAG chain acting as a surface to capture the interacting partners). Similarly, on the cell surfaces, HS proteoglycans increase the rate of growth factor and receptor encounters by decreasing the dimensionality from 3-D to 2-D.

Polyelectrolyte interactions with proteins are dominated by electrostatics as signaled by the effects of pH and ionic strength depending on the linear charge density of the polyelectrolyte and the charge anisotropy of the protein, and the ionic strength tunes the strength of protein–PE binding. Non-monotonic ionic strength dependence, an additional indication of non-specific binding, was seen for both non-cognate and cognate–PE systems,[134,168] *e.g.* AT–low molecular weight heparin. In this system, maximum binding occurs at $5 < I < 30$ mM NaCl (Fig. 12), where the Debye length is close to the protein radius (indication of the combination of short range attraction and long range repulsion).[135]

Conventional GAG models that feature uniquely protein-specific embedded binding sites arise from the lock-and-key analogy for protein (host)–ligand (guest). Applying a similar

analogy to protein–GAG systems neglects the inversion of the host–guest relationship. However, in many studies, native GAG chains are replaced by low MW analogs, and the characterization of protein–oligoheparin chains is based on crystallography (Fig. 13),[271–273] docking or MD simulations.[274] The antithrombin–pentasaccharide model epitomizes this perspective, positing a distinctive sequence on the Hp chain that interacts specifically with AT,[275] *i.e.* a specific pentasaccharide is required to activate AT towards coagulation protease, FXa in the anticoagulation.

The pentasaccharide model is increasingly viewed as a "gross approximation", of limited applicability for GAG–protein interactions in general.[129,135,265,276] Studies of tightly bound MW heparin analogs can be misleading, because enthalpic contributions are overemphasized, while entropic contributions are underestimated.[277] Early views of specificity, *i.e.*, the nature of the role of the Hp/HS sequence in GF recognition, have been challenged by recent findings of "promiscuous" binding between highly sulfated GAG chains and growth factors. Catlow *et al.* showed that the interaction of hepatocyte growth factor/scatter factor (HGF/SF) with HS is dominated by electrostatics and that HS sulfate *density* affects the selectivity.[278] Krueger *et al.* found that various FGFs share the same binding domain on HS, affinity correlated with the level of sulfation.[279] Jastrebova *et al.* found correlation between overall *O*-sulfation levels and the stability of the FGF–receptor–HS.[280] Zhang *et al.* showed that the higher degree of sulfation on heparin chains is preferred in interleukin 7 (IL-7) interactions.[281] These findings point to charge complementarity between the protein and the related polyanion, *i.e.* "there is an intermediate specificity based on the gradient of electrostatic interactions that are a function of relative charge densities, in contrast to high conformationally based structure specificity".[282]

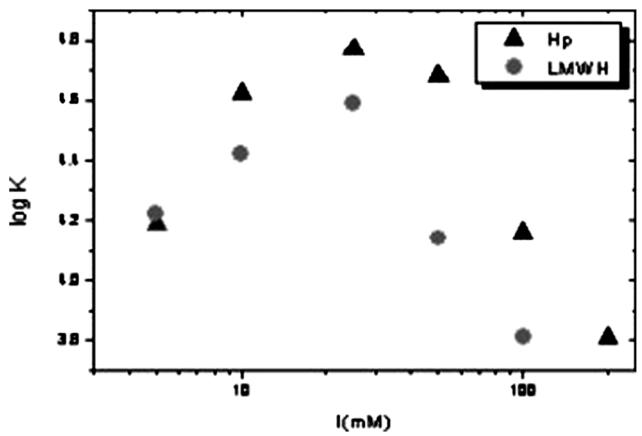

Fig. 12 The ionic strength dependence of the binding constant for AT–native heparin and low molecular weight heparin measured by FACCE at pH = 6.5. The binding constant was maximum at I = 25 mM for both.[135]

3.9 Protein–PE precipitation

Stoichiometric ([+]/[−] = 1) precipitates are formed from PE + protein in pure water and when Z_{pr} is large and opposite in sign to PE charge. Many studies have shown that PEs can precipitate proteins, but the molecular models of the precipitation process are still not clear. In general, the precipitation between PEs and proteins is recognized to be electrostatically driven. For example, Porfiri *et al.* reported that shielding by increasing ionic strength of the solution will lead to a reduction of precipitation.[283,284] Boeris reported that increasing ionic strength will reduce the efficiency of precipitation.[285] The same group studied concentration, ionic strength, and temperature effects to understand the mechanisms of precipitation between a strong polyanion (polyvinyl sulfonate) and positively charged protein (chymotrypsin) in the pH range 1–3.5. They proposed that precipitation was driven by the disorder of water molecules around the hydrophobic moieties of polymer chains.[18] Porfiri *et al.* showed that the phase diagram of α-amylase and PAA is sensitive to ionic strength and suggest that precipitation is likely to involve hydrophobic interactions between polymer and protein. Karayianni *et al.* recently found that coacervation, soluble complexation, and precipitation occur depending on a variety of conditions such as the charge ratio of PE–protein as shown in Fig. 14.[55] In addition, polymer molecular weight, protein charge, polymer charge density, and ionic strength also strongly affect the final state.[55] As the ionic strength was

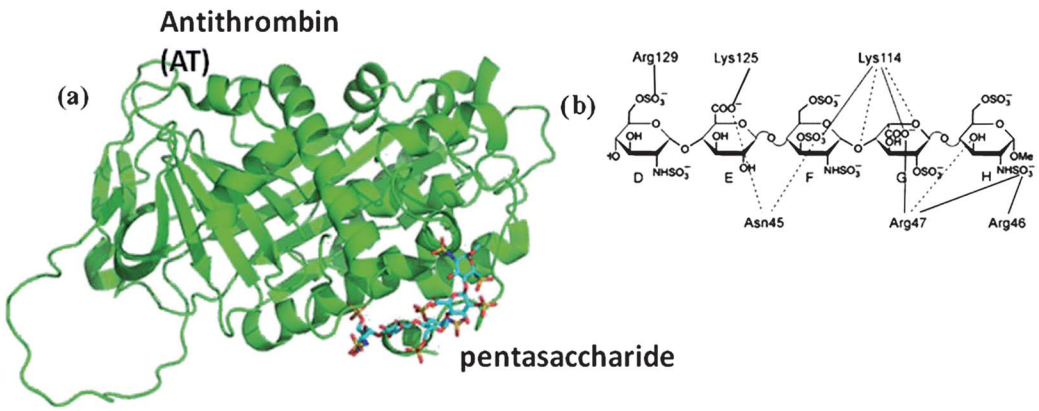

Fig. 13 (a) Crystal structure of AT and pentasaccharide; (b) the suggested hydrogen bonding (dashed lines) and salt bridges (solid lines) between AT residues and pentasaccharide charged groups.[271]

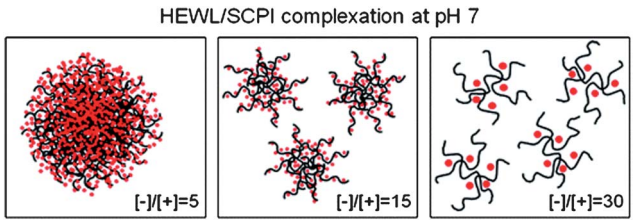

Fig. 14 Schematic representation of the structure of the formed complexes as a function of the charge ratio [−]/[+] for the HEWL/SCPI-54K systems at pH 7 and I = 0.01 M.[55]

increased, the electrostatic interaction is weakened leading to the aggregation of soluble complexes through hydrophobic interactions.[55] Tan *et al.* studied the precipitation of humic acid and protein complex at its isoelectric point and suggested that the hydrophobicity of humic acid likely plays an important role in the complex formation and precipitation.[286] As will be shown later, PE–protein precipitation has been widely applied to isolate or purify proteins.

4 Theory and simulations

4.1 Theory

Theories on the soluble complexes of oppositely charged macromolecules focus on linear (flexible, semi-flexible, rigid) polyelectrolytes and spherical or globular macroions. Increasing the rigidity of the polyelectrolyte chain results in undercharging of the complex.[287] In the case of strongly bound systems, *i.e.* highly charged macroions, Boroudjerdi and Netz[288] employed ground-state analysis, in which the fluctuations of the chain are neglected, to determine the configurations of the complexes between a semi-flexible worm-like chain and a semi-rigid sphere in the absence and presence of a salt. The parameters were taken from the DNA–histone system, and linear Debye–Huckel calculations were applied. The results indicate that transitions among configurational states, *i.e.* from wrapped to unwrapped, can be regulated by the sphere charge and salt concentration. At the lowest sphere charge, $Z = 12$, the maximum salt concentration at which the wrapped configuration still exists is 100 mM, close to the physiological salt concentration.

Schiessel[289] constructed a scaling theory for complexation at high and low salt concentrations. Prior to complete unbinding between a semi-flexible polyelectrolyte and oppositely charged spherical macroion, rosette-like structures (non-wrapped structures) can be seen. At high salt concentrations, when the screening is strong, a sharp transition from wrapped to rosette-like structure is seen with increasing chain stiffness. An influential paper by Nyugen and Shklovskii,[290] which was not cited in the previous review paper,[10] studied the complexation of long flexible polyelectrolytes with oppositely charged spherical particles in salt solutions (also see Section 3.6.4.). Under the effect of only electrostatic forces, a long PE molecule winds around oppositely charged spheres. The effect of charge inversion on the complexes was investigated with respect to the bulk concentration of the sphere and the polyelectrolyte. They demonstrated that when the charge of the protein–PE complex is close to zero, complexes condense together in bundles. A recent study by Cherstvy and Winkler[291] showed the scaling behavior of the critical conditions for weak adsorption of flexible polyelectrolytes to planar, cylindrical and spherical surfaces and the thickness of the adsorbed polymer nearby to the interface. At low salt conditions, the critical surface charge density (σ_c) scales as κ^3 for planar, κ^2 for cylindrical and κ^1 for spherical surfaces (Fig. 15), and this scaling trend was found to be consistent with PE–oppositely charged micelle complex formation experiments.

Protein–polyelectrolyte pH titrations indicate two critical pH values representing incipient binding (pH_c) and phase separation (pH_φ) (see Section 3.6.2.1). Below a critical salt concentration, the protein and polyelectrolyte can form soluble complexes, even though the protein has the same net charge as the polyelectrolyte. The complexation "on the wrong side" of the pI results from protein "charge patches" (see Section 3.1). To predict pH_c, on non-uniformly charged spheres, de Vries *et al.*[163] developed an analytical theory for the randomly charged surfaces. Theoretical calculations and experimental data on the complexation of gum Arabic, which was modeled as a single flexible chain of $N = 20$ charged hard spheres connected by harmonic springs, and whey protein isolate are found to be in agreement. Applying a similar nonuniform charge model to the whey proteins lactalbumin and lactoglobulin, the same author carried out Monte-Carlo simulations of their binding to weakly anionic gum Arabic. At their respective isoelectric points lactalbumin forms complexes more strongly than lactoglobulin, which was determined by the critical salt concentration below which soluble complexes can form on the wrong side of the protein's pI. The reason for this difference is due to one single positive "charge patch" on lactalbumin (consisting of a cluster of six positively charged groups), as opposed to multiple smaller charge patches on lactoglobulin.[292] Other models for the complexation of "wrong side of the pI" will be discussed further in the simulation section.

4.2 Simulation

Monte Carlo simulations of polyelectrolytes and oppositely charged macroion interactions contribute to the understanding

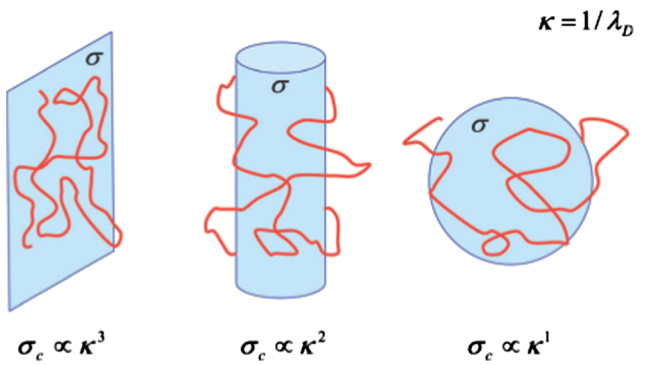

Fig. 15 The critical adsorption conditions represented for various surface geometries.[291]

of complex formation mechanisms and the effects of interaction parameters, such as chain stiffness, chain length, ionic concentration, and surface charge density. Johansson and Alstine[293] applied Monte Carlo simulations to investigate the driving forces for the adsorption of charged spherical proteins onto oppositely charged surface-grafted polymers. The adsorption mechanism is highly dependent on the critical surface charge density, which exhibits monotonic salt dependence, but does not depend on grafting density.

From some theoretical perspectives there is no difference between a nanoparticle and a protein. Monte Carlo simulations were also used to study the complexes between the polyelectrolyte and oppositely charged nanoparticles (NPs). The effects of ionic strength, NP surface charge density, PE intrinsic rigidity on the PE conformation and complex structure were investigated by Stoll and coworkers.[246] Complex structure is determined by the balance between attractive PE–NP interactions, and repulsive monomer/monomer and nanoparticle/nanoparticle interactions, which are also modulated by pH and ionic strength. The rigidity of the PE chain also has an impact on the number of NPs adsorbed, which is significantly less on flexible chains than on rodlike PEs.

Kayitmazer and coworkers[294] successfully applied full atomistic Monte Carlo simulations and electrostatic modeling (Delphi) for a protein (BSA) to show the importance of the charge complementarity between the protein and the polyelectrolyte to interact as shown in Fig. 16. In the simulations, the effect of anionic/nonionic copolymer charge distributions on the complexation with protein, which has distinct charge anisotropy, was investigated. The strongest binding was observed when the attractive and repulsive forces are optimized by the charge distribution of the polymer.

As noted in the theory section, PE-binding on the "wrong side of p*I*" has inspired many modeling efforts. Supplementing the theory mentioned above, de Vries[292] used coarse-grained Monte Carlo simulations to investigate the effect on the polyelectrolyte-binding strength of the distribution of protein charge patches at pH = p*I*. An existing theory for homopolymer adsorption on annealed random surfaces[295] was used taking into account protein excluded volume and approximating the electrostatic interaction energy between the protein and PE by Debye–Huckel potentials. A second effect "charge regulation" was clearly defined by de Vos *et al.*[173] An environment of high potential, *e.g.* a polyelectrolyte brush (see also Section 3.4) can effectively induce a change in p*I* and so bind a protein whose charge was originally of the same sign as the brush; this "charge regulation" can be differentiated from an interaction of the brush with densely and oppositely charged protein *structural* domains which overcomes the repulsion from the global like-charge protein. In their study, model proteins have the same net charge, but show different degrees of patchiness. The findings of de Vos *et al.*[173] show that patches with high charge density contribute more to binding.

In place of charge patches, Da Silva and co-workers[170] considered *induced* protein charge anisotropy as global charge fluctuations (capacitance) subject to perturbation by polyelectrolyte charge. Their charge regulation is defined as the ionization of essentially uniformly distributed weakly charged amino acid residues in the presence of a polyelectrolyte, and this can be quantified by the protein charge capacitance ($\langle Z^2\rangle - \langle Z\rangle^2$).[296] In addition, the effect of PE net charge on the dipole moment of the protein at pH = p*I* ("ion–dipole interaction") was taken into account. The polyelectrolyte was modeled as a single flexible chain of $N = 21$ charged hard spheres connected by harmonic springs. For three model proteins (lysozyme, α-lactalbumin and β-lactoglobulin), the charge regulation term was often stronger than the ion–dipole (several kTs). Da Silva and Jonsson[171] obtained similar results for albumin, goat and bovine α-lactalbumin, β-lactoglobulin, insulin, k-casein, lysozyme and pectin methylesterase, along with theoretical mutations.

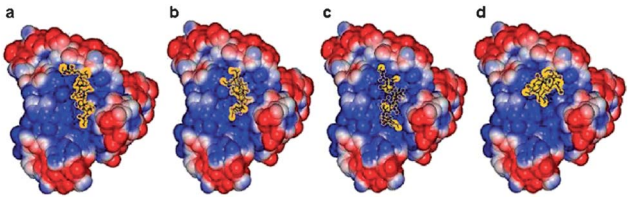

Fig. 16 Full-atom Monte Carlo simulation showing that the mobility of the bound synthetic polyanion resides on the positive domain of BSA, but never stops moving (I = 10 mM, pH = 6.8). Red and blue correspond to the negative and positive potentials, respectively, and they have been calculated using the nonlinear Poisson–Boltzmann equation. Each conformation corresponds to the minimized binding energy at given Monte Carlo steps: (a) 200k, (b) 400k, (c) 600k, and (d) 1000k MC steps.[294]

5 Applications

5.1 Protein stabilization

Formation of protein–polyelectrolyte complexes provides stabilization with respect to aggregation or amyloidogenesis, denaturation and enzymatic activity.

5.1.1 Inhibition of protein aggregation. Inhibition of protein aggregation might result from the formation of soluble complexes with PEs, because electrostatic repulsion between complexes can keep proteins from self-aggregating. Thus, heparin, a strong polyanion, binds to positively charged patches of insulin, and inhibits the electrostatic interactions among proteins themselves.[297] PEs have also been shown to control thermo-aggregation of proteins. Chung *et al.* found that dextran forms soluble complexes with partially unfolded BSA and prevents aggregation of denatured proteins upon heating.[298] Interestingly, the aggregation of β-lactoglobulin was significantly increased by chitosan in the pH range of 5.5–7.0, but the aggregation was suppressed by chitosan at pH 4.0.[299] Irina *et al.* found that both synthetic polyanions[300] and polycations[301] prevent thermoaggregation of the oligomeric enzymes (glyceraldehyde-3-phosphate dehydrogenase, lactate dehydrogenase, and aspartate aminotransferase). Further investigation by Stogov *et al.* indicated that hydrophilic high MW PEs efficiently inhibit thermo-aggregation without strongly influencing protein structure or enzyme activity.[302,303] In addition to inhibition of amorphous aggregation, PEs have been observed to reduce protein fibrillation. For example, Taluja and Bae found

that electrostatic complexation between PEG–poly(histine) and insulin could increase the solubility of insulin at pH 5.5 and subsequently reduce the fibrillation rate as shown in Fig. 17.[304] Tran *et al.* reported inhibition of amyloidogenesis of prion protein both *in vitro* and *in vivo* by PE multilayers coated by gold nanoparticles.[305]

5.1.2 Prevention of protein denaturation. PEs may also stabilize proteins against thermally induced denaturation. This effect is due to the elevation of protein melting temperature upon complexation with PEs. Properties such as hydrophobicity and charge density of PEs may still have a strong impact on the level of inhibition. Sedlák reported that negatively charged polymers with few hydrophobic groups barely affect the structure of proteins (chymotrypsinogen A, ribonuclease A, cytochrome c, lysozyme), but polyanions with more hydrophobic groups can induce irreversible structure perturbations.[306] This is consistent with the finding that dermatan sulfate is able to prevent BSA denaturation during the harsh microencapsulation process with poly(lactide-*co*-glycolide).[307] The critical denaturation temperature (T_{cd}) of recrystallized bacterial S-layers is increased by *ca.* 10 °C on PE multilayers relative to denaturation in solution[80] and poly(styrenesulfonate) destabilizes myoglobin by lowering its denaturation temperature.[308]

5.1.3 Preservation of enzyme activity. An increasing number of studies have focused on preservation of activity of enzymes incorporated in PE complexes for drug delivery purposes. It has been reported that activity can be largely preserved by enzymes immobilized on spherical PE brushes.[309] Gormally *et al.* also showed activity was retained when tyrosinase was immobilized on polycationic films.[79] When horseradish peroxidase is incorporated into chitosan complexes, the activity is also largely retained.[310] Saburova *et al.* studied the effects of polycation charge states and monomer structure on the stabilization of urease activity and observed that polycations can preserve enzyme activity but this was not observed for polyallylamine because the cation-binding sites were found to regulate the enzyme activity.[311] Hamlin *et al.* also showed that inhibition of β-galactosidase activity by the polyanion poly[1-[4-(3-carboxy-4-hydroxyphenylazo) benzenesulfonamido]-1,2-ethanediyl sodium salt] (PAZO) compared with the polycation poly(ethylenimine), suggesting enhanced stabilization of enzyme conformation by the polycation.[81] The enzymatic activity of chymotrypsin was increased by complexation with polyvinyl sulfonate and poly(acrylic acid).[312] On the other hand, the enzymatic activity of Hl-lipase embedded in complex micelles of poly-2-methylvinylpyridinium-co-poly(ethylene oxide) ($P2MVP_{41}$–PEO_{205}) and poly(acrylic acid) (PAA_{139}) was found to be increased.[42] This preservation effect is more obvious in the presence of non-ionic polymers, as shown by Marin *et al.* for polyphosphazene in stabilization of horseradish–peroxidase activity.[313] Control of protein aggregation is possible when experimental conditions (pH, ionic strength, temperature) required for soluble complex formation are determined.

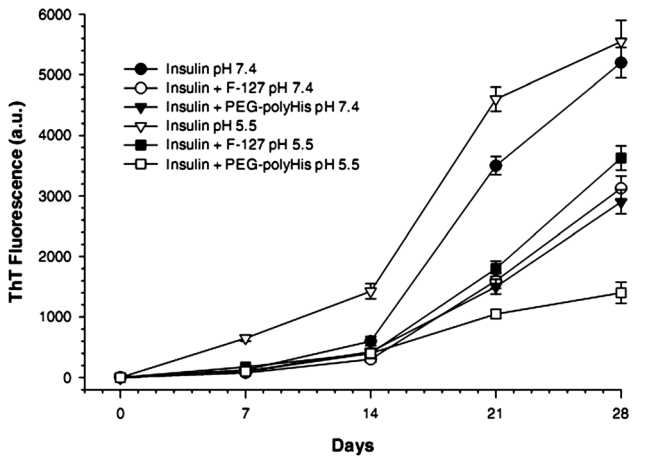

Fig. 17 Kinetics of fibrillation of insulin (initial concentration: ~1.0 mg mL^{-1}, n = 3) under different incubation conditions and/or on addition of PEG–polyHis (2.0 mg mL^{-1}) or F-127 (2.0 mg mL^{-1}).[304]

5.2 Separation/purification of proteins

Polyelectrolytes can be used to recover target proteins from their mixtures by (a) phase separation (precipitation or coacervation) or (b) by PE-modified substrates with selectivity comparable to chromatography; however questions persist about the degree of selectivity attainable through non-specific electrostatics. Bassani *et al.* reported precipitation of lipase from *C. rugosa* extracts and from a crude porcine pancreas. Purification factors for the extract were higher, suggesting low selectivity even though an increase of enzyme percentage was observed in the precipitate than in the extract.[314] Boeris *et al.* obtained a 4.7-fold increase in specific activity when polyvinyl sulfonate was used to recover chymotrypsin from a crude filtrate of bovine pancreas homogenate.[315] Zhang *et al.* obtained only low selectivity when poly(ethyleneimine) (PEI) precipitation was used as a fractionation and pre-concentration step before chromatographic methods to purify an acidic protein, recombinant β-glucuronidase (rGUS).[316] However, this technique primarily based on electrostatics, can efficiently separate proteins or remove impurities. Xu *et al.* showed selective coacervation of BLG isoform (BLG-A) by PDADMAC from a BLG-A–B mixture (Fig. 18) explained by the stronger binding affinity of BLG-A to the polycation.[174] Lysozyme could be purified from a transgenic tobacco extract by PE precipitation.[317] McDonald *et al.* showed that polyanion/polycation precipitation could replace cation/anion exchange chromatography as an initial or intermediate purification step in selective purification of monoclonal antibodies from host cell impurities such as host cell proteins (HCP), DNA, leached protein A, and antibody fragments and aggregates. pH, ionic strength, molecular weight, and protein pI were found to be important factors in selectivity and recovery yield.[318] Boeris *et al.* obtained pepsin with a purification factor of 9.0 using chitosan precipitation combined with two phase aqueous phase extraction.[319] Even higher selectivity can be obtained on PE modified substrates as shown by Aravind *et al.* who studied chitosan/polystyrene sulfonate multilayer coated membranes at pH 8.8, through which 100% of ovalbumin is permeated while 98% of lysozyme is rejected. In the permeation of these proteins, electrostatic interactions between proteins

and membrane PE layers were found to be more significant than the size.[320]

5.3 Protein delivery

The formation and dissolution of protein–PE complexes are sensitive to the pH and ionic strength conditions during encapsulation and release of a target protein. For example, many complexes will undergo swelling at extreme pHs. These properties can be used to trigger the release of proteins upon ingestion when complexes are exposed to the highly acidic digestive fluid. *In vitro* release studies are also conducted at ionic strength on the order of physiological salt concentrations. The structure of protein–PE complexes also plays a critical role in dictating the mechanisms of both uptake and the subsequent rate of delivery in the desired environment. These systems have been tested both *in vitro* and in simple *in vivo* models.

5.3.1 pH and ionic strength effects. Proteins are most easily released from positively charged PEs upon exposure to low pH upon ingestion. This is because of repulsive electrostatic interactions between polycations and proteins far below p*I*. LbL assembly immobilizes and encapsulates bioactive proteins, for example, release of enzymes from degradable PE capsules.[181] Complexes of positively charged trimethylchitosan (TMC) and PEG-ylated TMC with negatively charged insulin have been used to form positively charged complexes at low ionic strength and at pH 7.4 (pH > p*I*) (Fig. 19). In this case, excess polycations in the complexes prevent both thermal and enzymatic degradation of insulin.[93] The resulting release behavior and colloidal stability of the complexes were evaluated at low pH (<2) and at pH 6.8 in order to mimic both digestive and intestinal pH values.[93] Immediate dissolution and release of insulin at pH 2, but not at pH 6.8, resulted from repulsion between highly positive insulin and the positively charged chitosan derivatives.[93]

Alginate-based insulin nanoparticles have been shown to be capable of releasing proteins at intestinal pH.[321] Similarly, PE nanoparticles assembled from water soluble chitosan (WSC) and poly(aspartic acid) have been used for controlled release of BSA at physiological pH and at two acidic pHs, showing an initial burst followed by gradual protein release over 24 hours.[322] Complexes of alginate and chemically modified carboxymethyl chitosan were loaded with both BSA and lysozyme, with efficient release observed at elevated/physiological temperature, and desirable swelling behavior and subsequent release of proteins occur at low pH.[323] Solution pH was also shown to be critical for the stability of insulin–PE complexes. Studies on calcium-carboxymethyl chitosan hydrogel beads have shown formation of stable complexes with BSA, and release at low pH due to swelling of the resultant protein–PE complexes.[225] Polyelectrolyte complex (PEC) beads made from chitosan–alginate mixtures show protein release behavior that is highly dependent on both complex pH and stoichiometry.[260] Ternary complexes of WSC and poly(α,β-L-malic acid), PMA, complexed with insulin aggregates, are subsequently disrupted by either lowering the pH or increasing *I*, resulting in release of bioactive insulin.[113] This release, best characterized as a "burst" was later found to be modulated by increasing the number of PE layers.[113] Polyacrylic acid–lysozyme microgels form core–shell particles, where slow exchange of lysozyme from particles results in gradual protein release. The release of lipase from PE vesicles is dependent on the ionic strength, *i.e.* high ionic strengths – on the order of physiological salt concentrations – trigger near instantaneous disassembly of the PE micelles, resulting in the release of proteins due to disruption of attractive electrostatic forces.[42] Conversely when salt concentrations are decreased, the release of lysozyme becomes even slower due to increased attractive interactions.[107]

5.3.2 Effects of structure and morphology. The morphology of PE–protein complexes can be controlled, resulting in the formation of hollow cavities or core–shell structures from which protein can gradually diffuse away once desired release conditions are achieved. The release profiles of BSA-loaded PEMs can be tuned by varying the composition of the particle shell

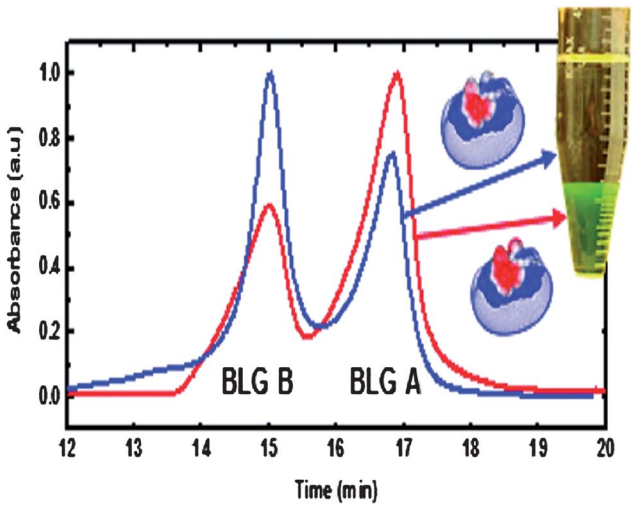

Fig. 18 Ion exchange chromatography analysis of BLG-A and -B composition in different phases after PE coacervation of native BLG (A : B ~ 1 : 1). Red line: coacervate, blue line: supernatant.[174]

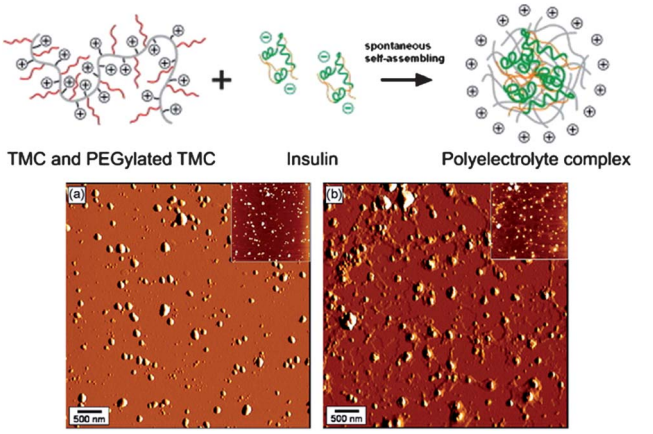

Fig. 19 Top: schematic representation of insulin polyelectrolyte complex formation. Bottom: atomic force microscopy images (5 μm × 5 μm) of: (a) TMC400–insulin PEC at an optimal polymer–insulin mass ratio of 0.3 : 1 and (b) TMC400–insulin PEC at a polymer–insulin mass ratio of 1 : 1.[93]

showing that formulation of such complexes can dictate the rate of dissolution.[99] The concentration of lysozyme is presumed to be higher in the shell for core–shell particles formed from PAA microgels.[324] These structures sequester protein in outer layers making it easier for the salt to trigger the release of protein.[324] LbL films can be tuned for gradual release of insulin by varying PE stoichiometry, resulting in systems capable of both controlled release, selective permeability, and to some extent protection from enzymatic degradation.[142] It was speculated that coupling with protease inhibitors would allow for formulation of looser complexes that would permit more gradual release.[142] The high water content of lipase filled PE vesicles has been shown to be necessary to preserve enzyme activity.[42] Another possible morphology is hollow biodegradable PE capsules, made in this case from cysteamine conjugated chitosan and dextran sulfate.[141] These capsules show controlled release of BSA from within their inner compartments at low pH allowing for swelling of the complex and subsequent diffusion of protein.[141]

5.3.3 Studies in biological systems. PE–protein complexes have been tested in organisms, or in cell or tissue culture. PE-based multilayers effectively deliver growth factors in cell culture without denaturation or disruption of native fibroblast growth factor (FGF) or cytotoxicity.[102] The effectiveness of insulin-loaded alginate–chitosan nanoparticles in regulating serum glucose levels after oral delivery of nanoparticles to diabetic rats indicates not only effective delivery and release, but also preservation of bioactivity of insulin.[97] PEMs assembled from dextran sulfate and poly(arginine) at physiological pH have been shown to have desirable release behavior when complexed with OVA peptide (an epitope of ovalbumin), capable of delivering a target peptide in two different tissue types.[325]

6 Conclusion and outlook

The field of protein–polyelectrolyte interactions is developing rapidly but in a somewhat balkanized way, so we have attempted to present an inclusive picture of activities coming from *viz.* food science, drug delivery, biosensors and separations. The questions asked focus on the nature of the binding energetics, the structure and properties of the resultant states, and their application-dependent "functionality". The paradigms themselves are highly discipline-dependent: from the biochemical point of view, proteins are structurally complex and versatile actors in the ecology of life, so that perturbation of structure and function upon complexation is presumed to be the case. In contrast, as components with polyelectrolytes in new materials and devices, they appear to be remarkably robust. Whether this contradiction arises simply from the nature of the proteins chosen for non-physiological purposes is not yet clear. Biochemically oriented studies rarely stray from physiological pH and ionic strength, two parameters absolutely central from the physico-chemical, materials or assembly perspectives.

Future work will involve both extending the range of protein–polyelectrolyte pairs examined, and developing fundamental insights of broad relevance. The number of systems described in the extensive bibliography of this review is in fact a small sampling of possible ones. This is not just due to the number of polyelectrolyte–protein pairs and their phase states, but also to the varied architectures of polyelectrolyte assemblies, including adsorbed monolayers, multilayers, brushes, nanoparticles and gels. These lead to numerous modes of protein complexation with applications in biosensing, enzyme immobilization, and the containment and delivery of protein drugs. While general rules for structures and properties are emerging, considerations of effects on different length scales are not well integrated. The fundamental electrostatics governing protein–polyelectrolyte binding affinity may arise from a local protein charge and the charge density and local flexibility of the corresponding polyelectrolyte chain sequence. However, a general understanding of "local" has not appeared. The broad applicability of binding isotherm models such as McGhee–von Hippel has not been established, and few studies compare thermodynamic parameters extracted from calorimetry with those obtained from binding isotherms based on other methods. Most prominently, the transferability to polyelectrolyte–protein systems of models derived by Manning in the context of oligolysine–DNA interactions has been questioned.[326]

Also not well integrated are the two general categories of complex coacervation: polyelectrolyte–colloid and polyelectrolyte–polyelectrolyte. When system polydispersity is minimized, the former appears to show phenomenologically well-defined micro- or macro-phase transitions that can be induced by changes in the charge of the colloid, the charge of the polyelectrolyte, the ionic strength, or the system stoichiometry. Reports of such discontinuities for polyelectrolyte–polyelectrolyte systems are rarely based on direct observation, but instead involve mixing of the two polyions at fixed conditions of, *e.g.*, ionic strength, polyelectrolyte charge or stoichiometry, and so may be susceptible to local concentration variations. Dependence of the final state on the mode of addition is rarely examined. For several reasons, minimizing system polydisperity in PE–PE systems is generally more challenging, so such studies should be done with narrow MWD polymers of fixed as opposed to labile charges to minimize disproportionation.

Polyelectrolyte–colloid systems are intermediate between the fields of polyelectrolyte surface adsorption and polyelectrolyte ion-binding (*viz.* is a "generation 2" dendrimer a small colloid particle or a large counterion? Is there a radius of curvature defining the separation between binding of polyelectrolytes to planar *vs.* spherical surfaces?). The concept of a critical pH for protein–polyelectrolyte complexation "pH_c" that has become common is essentially based on theories for critical conditions for the binding of polyelectrolytes to oppositely charged surfaces as described in Section 4, most recently discussed and extended by Cherstvy and Winkler.[291] Experimentally, pH_c is detectable as a discontinuity in the derivative of some measurable property with respect to pH, *i.e.* a second-order transition, so its nature should be clarified. "pH_ϕ" appears to be a true phase transition, but both of these "critical" points can be broadened beyond recognition by polydispersity, making the convergence of theory and experiment more elusive. In any event, the "maps" or "boundaries" that appear for both of these putative transitions may elude efforts to identify them as phase

diagrams. Even when one variable is a macromolecular concentration, the interchange or disproportionation among macromolecular complexes can rule out the application of tie-lines.

References

1 H. Morawetz and W. L. Hughes, *J. Phys. Chem.*, 1952, **56**, 64.
2 M. Berdick and H. Morawetz, *J. Biol. Chem.*, 1954, **206**, 959.
3 H. Morawetz and H. Sage, *Arch. Biochem. Biophys.*, 1955, **56**, 103.
4 A. A. Green and W. L. Hughes, *Methods Enzymol.*, 1955, **1**, 67.
5 R. V. Rice, M. A. Stahmann and R. A. Alberty, *J. Biol. Chem.*, 1954, **209**, 105.
6 P. Bernfeld, V. M. Donahue and M. E. Berkowitz, *J. Biol. Chem.*, 1957, **226**, 51.
7 W. M. McKernan and C. R. Ricketts, *Biochem. J.*, 1960, **76**, 117.
8 C. S. Patrickios, W. R. Hertler and T. A. Hatton, *Biotechnol. Bioeng.*, 1994, **44**, 1031.
9 P. L. Dubin, J. Gao and K. Mattison, *Sep. Purif. Methods*, 1994, **23**, 1.
10 C. L. Cooper, P. L. Dubin, A. B. Kayitmazer and S. Turksen, *Curr. Opin. Colloid Interface Sci.*, 2005, **10**, 52.
11 S. L. Turgeon, C. Schmitt and C. Sanchez, *Curr. Opin. Colloid Interface Sci.*, 2007, **12**, 166.
12 A. L. Becker, K. Henzler, N. Welsch, M. Ballauff and O. Borisov, *Curr. Opin. Colloid Interface Sci.*, 2012, **17**, 90.
13 R. de Vries and M. C. Stuart, *Curr. Opin. Colloid Interface Sci.*, 2006, **11**, 295.
14 S. Ulrich, M. Seijo and S. Stoll, *Curr. Opin. Colloid Interface Sci.*, 2006, **11**, 268.
15 E. Kokufuta, H. Shimizu and I. Nakamura, *Polym. Bull.*, 1980, **2**, 157.
16 L. S. Ahmed, J. L. Xia, P. L. Dubin and E. Kokufuta, *J. Macromol. Sci., Pure Appl. Chem.*, 1994, **A31**, 17.
17 M. A. Hiroshi, R. Kikuchi, K. Ogawa and E. Kokufuta, *Colloids Surf., B*, 2007, **56**, 142.
18 V. Boeris, D. Spelzini, J. P. Salgado, G. Picó, D. Romanini and B. Farruggia, *Biochim. Biophys. Acta*, 2008, **1780**, 1032.
19 E. Serefoglou, J. Oberdisse and G. Staikos, *Biomacromolecules*, 2007, **8**, 1195.
20 E. Raspaud, I. Chaperon, A. Leforestier and F. Livolant, *Biophys. J.*, 1999, **77**, 1547.
21 M. Antonov, M. Mazzawi and P. L. Dubin, *Biomacromolecules*, 2010, **11**, 51.
22 B. Sperber, H. A. Schols, M. A. C. Stuart, W. Norde and A. G. J. Voragen, *Food Hydrocolloids*, 2009, **23**, 765.
23 S. A. Tikhonenko, E. A. Saburova, E. N. Durdenko and B. I. Sukhorukov, *Russ. J. Phys. Chem. A*, 2009, **83**, 1781.
24 P. J. Flory. *Principles of Polymer Chemistry*, Cornell University Press, Ithaca, 1953.
25 Y. Xu, D. Seeman, Y. Yan, L. Sun, J. Post and P. L. Dubin, *Biomacromolecules*, 2012, **13**, 1642.
26 P. R. Majhi, R. R. Ganta, R. P. Vanam, E. Seyrek, K. Giger and P. L. Dubin, *Langmuir*, 2006, **22**, 9150.
27 K. Y. Wang and B. I. Kurganov, *Biophys. Chem.*, 2003, **106**, 97.
28 Y. Xu, Y. Yan, D. Seeman, L. Sun and P. L. Dubin, *Langmuir*, 2011, **28**, 579.
29 M. H. Smith and L. A. Lyon, *Macromolecules*, 2011, **44**, 8154.
30 S. I. Laneuville, S. L. Turgeon, C. Sanchez and P. Paquin, *Langmuir*, 2006, **22**, 7351.
31 S. I. Laneuville, C. Sanchez, S. L. Turgeon, S. L. J. Hardy and P. Paquin., *Food Colloids: Interactions, Microstructure and Processing*, 2005, p. 443.
32 A. B. Kayitmazer, H. B. Bohidar, K. W. Mattison, A. Bose, J. Sarkar, A. Hashidzume, P. S. Russo, W. Jaeger and P. L. Dubin, *Soft Matter*, 2007, **3**, 1064.
33 A. B. Kayitmazer, S. P. Strand, C. Tribet, W. Jaeger and P. L. Dubin, *Biomacromolecules*, 2007, **8**, 3568.
34 E. Kizilay, A. B. Kayitmazer and P. L. Dubin, *Adv. Colloid Interf.*, 2011, **167**, 24.
35 V. Boeris, Y. Micheletto, M. Lionzo, N. P. da Silveira and G. Pico, *Carbohyd. Polym.*, 2011, **84**, 459.
36 Y. C. Tang, J. C. Duan and J. H. Wu, *Colloids Surf., A*, 2012, **395**, 82.
37 J. Gummel, F. Boue, D. Clemens and F. Cousin, *Soft Matter*, 2008, **4**, 1653.
38 F. Cousin, J. Gummel, S. Combet and F. Boué, *Adv. Colloid Interf.*, 2011, **167**, 71.
39 F. Cousin, J. Gummel, D. Clemens, I. Grillo and F. Boue, *Langmuir*, 2010, **26**, 7078.
40 F. Cousin, J. Gummel, D. Ung and F. Boue, *Langmuir*, 2005, **21**, 9675.
41 J. Gummel, F. Cousin, J. M. Verbavatz and F. Boue, *J. Phys. Chem. B*, 2007, **111**, 8540.
42 S. Lindhoud, R. de Vries, R. Schweins, M. A. C. Stuart and W. Norde, *Soft Matter*, 2009, **5**, 242.
43 I. Schmidt, F. Cousin, C. Huchon, F. Boue and M. A. V. Axelos, *Biomacromolecules*, 2009, **10**, 1346.
44 J. Gummel, F. Cousin and F. Boue, *Macromolecules*, 2008, **41**, 2898.
45 I. Schmidt, B. Novales, F. Boue and M. A. V. Axelos, *J. Colloid Interface Sci.*, 2010, **345**, 316.
46 S. Chodankar, V. K. Aswal, J. Kohlbrecher, R. Vavrin and A. G. Wagh, *Phys. Rev. E: Stat., Nonlinear, Soft Matter Phys.*, 2008, **78**.
47 S. Lindhoud, L. Voorhaar, R. de Vries, R. Schweins, M. A. C. Stuart and W. Norde, *Langmuir*, 2009, **25**, 11425.
48 I. Morfin, I. Grillo, E. Buhler, F. Cousin and F. Boue, *Biomacromolecules*, 2011, **12**, 859.
49 V. Ball and C. Maechling, *Int. J. Mol. Sci.*, 2009, **10**, 3283.
50 C.-Y. Hsu, H.-Y. Lin, J. L. Thomas, B.-T. Wu and T.-C. Chou, *Biosens. Bioelectron.*, 2006, **22**, 355.
51 H. i. K. S. Souza, M. d. P. Gonçalves and J. Gómez, *Biomacromolecules*, 2011, **12**, 1015.
52 D. S. Bastos, B. N. Barreto, H. K. S. Souza, M. Bastos, M. H. M. Rocha-Leão, C. T. Andrade and M. P. Gonçalves, *Food Hydrocolloids*, 2010, **24**, 709.
53 G. Baier, C. Costa, A. Zeller, D. Baumann, C. Sayer, P. H. H. Araujo, V. Mailänder, A. Musyanovych and K. Landfester, *Macromol. Biosci.*, 2011, **11**, 628.

54 K. Chen, Y. Xu, S. Rana, O. R. Miranda, P. L. Dubin, V. M. Rotello, L. Sun and X. Guo, *Biomacromolecules*, 2011, **12**, 2552.
55 M. Karayianni, S. Pispas, G. D. Chryssikos, V. Gionis, S. Giatrellis and G. Nounesis, *Biomacromolecules*, 2011, **12**, 1697.
56 D. Romanini, M. Braia, R. G. Angarten, W. Loh and G. Picó, *J. Chromatogr., B: Anal. Technol. Biomed. Life Sci.*, 2007, **857**, 25.
57 M. Braia, M. C. Porfiri, B. Farruggia, G. Picó and D. Romanini, *J. Chromatogr., B: Anal. Technol. Biomed. Life Sci.*, 2008, **873**, 139.
58 M. Braia, G. Tubio, B. Nerli, W. Loh and D. Romanini, *Int. J. Biol. Macromol.*, 2012, **50**, 180.
59 N. Welsch, A. L. Becker, J. Dzubiella and M. Ballauff, *Soft Matter*, 2012, **8**.
60 K. Henzler, B. Haupt, K. Lauterbach, A. Wittemann, O. Borisov and M. Ballauff, *J. Am. Chem. Soc.*, 2010, **132**, 3159.
61 A. L. Becker, N. Welsch, C. Schneider and M. Ballauff, *Biomacromolecules*, 2011, **12**, 3936.
62 K. Laos, R. Parker, J. Moffat, N. Wellner and S. G. Ring, *Carbohyd. Polym.*, 2006, **65**, 235.
63 R. Dronov, D. G. Kurth, H. Möhwald, F. W. Scheller and F. Lisdat, *Electrochim. Acta*, 2007, **53**, 1107.
64 M. Futamura, P. Dhanasekaran, T. Handa, M. C. Phillips, S. Lund-Katz and H. Saito, *J. Biol. Chem.*, 2005, **280**, 5414.
65 A. Kusumo, L. Bombalski, Q. Lin, K. Matyjaszewski, J. W. Schneider and R. D. Tilton, *Langmuir*, 2007, **23**, 4448.
66 H.-S. Kim, S.-H. Jung, S.-H. Kim, I.-B. Suh, W. J. Kim, J.-W. Jung, J. s. Yuk, Y.-M. Kim and K.-S. Ha, *Proteomics*, 2006, **6**, 6426.
67 H. Vaisocherová, W. Yang, Z. Zhang, Z. Cao, G. Cheng, M. Piliarik, J. i. Homola and S. Jiang, *Anal. Chem.*, 2008, **80**, 7894.
68 N. Akkilic, M. Mustafaev and V. Chegel, *Macromol. Symp.*, 2008, **269**, 138.
69 J. Watanabe, H. Shen and M. Akashi, *Acta Biomater.*, 2008, **4**, 1255.
70 M. C. Dixon, *J. Biomol. Tech.*, 2008, **19**, 151.
71 H. Y. Liu and N. F. Hu, *J. Phys. Chem. B*, 2006, **110**, 14494.
72 Q. Li, J. F. Quinn, Y. Wang and F. Caruso, *Chem. Mater.*, 2006, **18**, 5480.
73 S. Channasanon, W. Graisuwan, S. Kiatkamjornwong and V. P. Hoven, *J. Colloid Interface Sci.*, 2007, **316**, 331.
74 W. Guo and N. Hu, *Biophys. Chem.*, 2007, **129**, 163.
75 K. Uto, K. Yamamoto, N. Kishimoto, M. Muraoka, T. Aoyagi and I. Yamashita, *J. Mater. Chem.*, 2008, **18**, 3876.
76 H. Yao, X. Guo and N. Hu, *Electrochim. Acta*, 2009, **54**, 7330.
77 M. Lundin, U. M. Elofsson, E. Blomberg and M. W. Rutland, *Colloids Surf., B*, 2010, **77**, 1.
78 C. Kepplinger, F. Lisdat and U. Wollenberger, *Langmuir*, 2011, **27**, 8309.
79 M. V. Gormally, R. K. McKibben, M. S. Johal and C. R. D. Selassie, *Langmuir*, 2009, **25**, 10014.
80 M. Delcea, R. Krastev, T. Gutberlet, D. Pum, U. B. Sleytr and J. L. Toca-Herrera, *Soft Matter*, 2008, **4**, 1414.
81 R. E. Hamlin, T. L. Dayton, L. E. Johnson and M. S. Johal, *Langmuir*, 2007, **23**, 4432.
82 G. V. Martins, E. G. Merino, J. F. Mano and N. M. Alves, *Macromol. Biosci.*, 2010, **10**, 1444.
83 J. Borges, J. M. Campina, H. K. S. Souza, M. P. Goncalves and A. F. Silva, *Soft Matter*, 2012, **8**.
84 E. Reimhult, C. Larsson, B. Kasemo and F. Höök, *Anal. Chem.*, 2004, **76**, 7211.
85 E. Bittrich, K. B. Rodenhausen, K. J. Eichhorn, T. Hofmann, M. Schubert, M. Stamm and P. Uhlmann, *Biointerphases*, 2010, **5**, 1.
86 E. M. Pinto, M. M. Barsan and C. M. A. Brett, *J. Phys. Chem. B*, 2010, **114**, 15354.
87 B. Mohanty, A. Gupta, H. B. Bohidar and S. Bandyopadhyay, *J. Polym. Sci., Part B: Polym. Phys.*, 2007, **45**, 1511.
88 Y. Du, C. G. Chen, B. L. Li, M. Zhou, E. K. Wang and S. J. Dong, *Biosens. Bioelectron.*, 2010, **25**, 1902.
89 W. Y. Yuan, H. Dong, C. M. Li, X. Q. Cui, L. Yu, Z. S. Lu and Q. Zhou, *Langmuir*, 2007, **23**, 13046.
90 A. Nadiri, S. Kuchler-Bopp, H. Mjahed, B. Hu, Y. Haikel, P. Schaaf, J. C. Voegel and N. Benkirane-Jessel, *Small*, 2007, **3**, 1577.
91 J. M. Campiña, H. K. S. Souza, J. Borges, A. Martins, M. P. Gonçalves and F. Silva, *Electrochim. Acta*, 2010, **55**, 8779.
92 S. R. Mao, U. Bakowsky, A. Jintapattanakit and T. Kissel, *J. Pharm. Sci.*, 2006, **95**, 1035.
93 A. Jintapattanakit, V. B. Junyaprasert, S. Mao, J. Sitterberg, U. Bakowsky and T. Kissel, *Int. J. Pharm.*, 2007, **342**, 240.
94 R. Dronov, D. G. Kurth, H. Mohwald, F. W. Scheller, J. Friedmann, D. Pum, U. B. Sleytr and F. Lisdat, *Langmuir*, 2008, **24**, 8779.
95 G. Olanya, E. Thormann, I. Varga, R. Makuška and P. M. Claesson, *J. Colloid Interface Sci.*, 2010, **349**, 265.
96 N. S. Claxton; T. J. Fellers and M. W. Davidson, In *Encyclopedia of Medical Devices and Instrumentation*, John Wiley & Sons, Inc., 2006.
97 B. Sarmento, A. Ribeiro, F. Veiga, P. Sampaio, R. Neufeld and D. Ferreira, *Pharm. Res.*, 2007, **24**, 2198.
98 C. M. Jewell, S. M. Fuchs, R. M. Flessner, R. T. Raines and D. M. Lynn, *Biomacromolecules*, 2007, **8**, 857.
99 Z. She, M. N. Antipina, J. Li and G. B. Sukhorukov, *Biomacromolecules*, 2010, **11**, 1241.
100 O. Kreft, M. Prevot, H. Mohwald and G. B. Sukhorukov, *Angew. Chem., Int. Ed.*, 2007, **46**, 5605.
101 H. Lee, Y. Jeong and T. G. Park, *Biomacromolecules*, 2007, **8**, 3705.
102 Y. Itoh, M. Matsusaki, T. Kida and M. Akashi, *Biomacromolecules*, 2008, **9**, 2202.
103 Y. Li, Z. Zhang, H. P. van Leeuwen, M. A. Cohen Stuart, W. Norde and J. M. Kleijn, *Soft Matter*, 2011, **7**, 10377.
104 S. H. Liu, Y. L. Cao, S. Ghosh, D. Rousseau, N. H. Low and M. T. Nickerson, *J. Agric. Food Chem.*, 2010, **58**, 552.
105 W. Park and K. Na, *Colloids Surf., B*, 2009, **72**, 193.
106 T. Crouzier, K. Ren, C. Nicolas, C. Roy and C. Picart, *Small*, 2009, **5**, 598.

107 C. Johansson, P. Hansson and M. Malmsten, *J. Colloid Interface Sci.*, 2007, **316**, 350.
108 Y. Li, J. M. Kleijn, M. A. Cohen Stuart, T. Slaghek, J. Timmermans and W. Norde, *Soft Matter*, 2011, **7**.
109 Y. Li, W. Norde and J. M. Kleijn, *Langmuir*, 2011, **28**, 1545.
110 L. Bayes-Garcia, L. Ventola, R. Cordobilla, R. Benages, T. Calvet and M. A. Cuevas-Diarte, *Sol. Energy Mater. Sol. Cells*, 2010, **94**, 1235.
111 C. L. de Vasconcelos, P. M. Bezerril, T. N. C. Dantas, M. R. Pereira and J. L. C. Fonseca, *Langmuir*, 2007, **23**, 7687.
112 B. Sarmento, D. Ferreira, F. Veiga and A. Ribeiro, *Carbohydr. Polym.*, 2006, **66**, 1.
113 Y. F. Fan, Y. N. Wang, Y. G. Fan and J. B. Ma, *Int. J. Pharm.*, 2006, **324**, 158.
114 J. Guo, Y. Zhang and X. Q. Yang, *Food Hydrocolloids*, 2012, **26**, 277.
115 Y. A. Antonov and P. Moldenaers, *Food Hydrocolloids*, 2011, **25**, 350.
116 N. Rodthongkum, R. Ramireddy, S. Thayumanavan and W. V. Richard, *Analyst*, 2012, **137**, 1024.
117 N. Rodthongkum, Y. Chen, S. Thayumanavan and R. W. Vachet, *Anal. Chem.*, 2010, **82**, 8686.
118 J. D. Dunn, E. A. Igrisan, A. M. Palumbo, G. E. Reid and M. L. Bruening, *Anal. Chem.*, 2008, **80**, 5727.
119 N. T. Kitagawa, *Anal. Chem.*, 2005, **78**, 459.
120 H. Kawasaki, T. Sugitani, T. Watanabe, T. Yonezawa, H. Moriwaki and R. Arakawa, *Anal. Chem.*, 2008, **80**, 7524.
121 E. Seyrek, T. Hattori and P. L. Dubin, *Methods Mol. Biol.*, 2004, **276**, 217.
122 A. Liang, X. He, Y. Du, K. Wang, Y. Fung and B. Lin, *J. Pharm. Biomed. Anal.*, 2005, **38**, 408.
123 L. Yi, L. Xiaomei, F. Hui, Z. Yingcheng, L. Dan and W. Ying, *J. Chromatogr., A*, 2007, **1143**, 284.
124 I. J. Colton, J. D. Carbeck, J. Rao and G. M. Whitesides, *Electrophoresis*, 1998, **19**, 367.
125 D. J. Winzor, *Anal. Biochem.*, 2008, **383**, 1.
126 J. McKeon and L. A. Holland, *Electrophoresis*, 2004, **25**, 1243.
127 M. N. Preising and S. Heegard, *Trends Mol. Med.*, 2004, **10**, 51.
128 A. Varenne, P. Gareil, S. Colliec-Jouault and R. Daniel, *Anal. Biochem.*, 2003, **315**, 152.
129 B. L. Henry, J. Connell, A. Liang, C. Krishnasamy and U. R. Desai, *J. Biol. Chem.*, 2009, **284**, 20897.
130 M. Anderot, M. Nilsson, A. Vegvari, E. H. Moeller, M. van de Weert and R. Isaksson, *J. Chromatogr., B: Anal. Technol. Biomed. Life Sci.*, 2009, **877**, 892.
131 J. Y. Gao, P. L. Dubin and B. B. Muhoberac, *Anal. Chem.*, 1997, **69**, 2945.
132 L. W. Nichol, W. J. Jackson and D. J. Winzor, *Biochemistry*, 1972, **11**, 585.
133 D. J. Winzor, *Anal. Biochem.*, 2006, **349**, 285.
134 T. Hattori, K. Kimura, E. Seyrek and P. L. Dubin, *Anal. Biochem.*, 2001, **295**, 158.
135 E. Seyrek, P. L. Dubin and J. Henriksen, *Biopolymers*, 2007, **86**, 249.
136 T. Le Saux, A. Varenne, F. Perreau, L. Siret, S. Duteil, L. Duhau and P. Gareil, *J. Chromatogr., A*, 2006, **1132**, 289.
137 S. Fermas, F. Gonnet, A. Varenne, P. Gareil and R. Daniel, *Anal. Chem.*, 2007, **79**, 4987.
138 W. C. Johnson, *Proteins: Struct., Funct., Genet.*, 1990, **7**, 205.
139 M. Muller, B. Kessler, N. Houbenov, K. Bohata, Z. Pientka and E. Brynda, *Biomacromolecules*, 2006, **7**, 1285.
140 B. Sarmento, D. C. Ferreira, L. Jorgensen and M. van de Weert, *Eur. J. Pharm. Biopharm.*, 2007, **65**, 10.
141 S. J. Shu, X. G. Zhang, Z. M. Wu, Z. Wang and C. X. Li, *Biomaterials*, 2010, **31**, 6039.
142 K. Yoshida, K. Sato and J. Anzai, *J. Mater. Chem.*, 2010, **20**, 1546.
143 B. L. H. M. Sperber, M. A. C. Stuart, H. A. Schols, A. G. J. Voragen and W. Norde, *Biomacromolecules*, 2009, **10**, 3246.
144 E. V. Kudryashova, A. J. W. G. Visser, A. van Hoek and H. H. J. de Jongh, *Langmuir*, 2007, **23**, 7942.
145 M. L. Davies, P. Douglas, H. D. Burrows, M. D. Miguel and A. Douglas, *J. Phys. Chem. B*, 2011, **115**, 6885.
146 Y. Tao and L. Zhang, *Carbohydr. Res.*, 2008, **343**, 2251.
147 S. Beeckmans, *Methods*, 1999, **19**, 278.
148 J. Xia and P. L. Dubin, *J. Chromatogr., A*, 1994, **667**, 311.
149 C. J. Robinson, N. J. Harmer, S. J. Goodger, T. L. Blundell and J. T. Gallagher, *J. Biol. Chem.*, 2005, **280**, 42274.
150 N. J. Harmer, C. J. Robinson, L. E. Adam, L. L. Ilag, C. V. Robinson, J. T. Gallagher and T. L. Blundell, *Biochem. J.*, 2006, **393**, 741.
151 M.-R. Park, C. Chun, C.-S. Cho and S.-C. Song, *Eur. J. Pharm. Biopharm.*, 2010, **76**, 179.
152 H. Bohidar, P. L. Dubin, P. R. Majhi, C. Tribet and W. Jaeger, *Biomacromolecules*, 2005, **6**, 1573.
153 S. S. Singh, V. K. Aswal and H. B. Bohidar, *Int. J. Biol. Macromol.*, 2007, **41**, 301.
154 W. Kopaciewicz, M. A. Rounds, J. Fausnaugh and F. E. Regnier, *J. Chromatogr.*, 1983, **266**, 3.
155 V. Lesins and E. Ruckenstein, *Colloid Polym. Sci.*, 1988, **266**, 1187.
156 M. A. Strege, P. L. Dubin, J. S. West and C. D. Flinta, *ACS Symp. Ser.*, 1990, **427**, 66.
157 R. D. Rosenberg, *Annu. Rev. Med.*, 1978, **29**, 367.
158 R. D. Rosenberg, *Semin. Hematol.*, 1977, **14**, 427.
159 A. Imberty, H. Lortat-Jacob and S. Perez, *Carbohydr. Res.*, 2007, **342**, 430.
160 D. J. Roush, D. S. Gill and R. C. Willson, *Biophys. J.*, 1994, **66**, 1290.
161 E. Boura and J. H. Hurley, *Proc. Natl. Acad. Sci. U. S. A.*, 2012, **109**, 1901.
162 Q. H. Ren and M. A. Gorovsky, *Mol. Cell. Biol.*, 2003, **23**, 2778.
163 R. de Vries, F. Weinbreck and C. G. de Kruif, *J. Chem. Phys.*, 2003, **118**, 4649.
164 T. Selzer, S. Albeck and G. Schreiber, *Nat. Struct. Biol.*, 2000, **7**, 537.
165 J. M. Park, B. B. Muhoberac, P. L. Dubin and J. L. Xia, *Macromolecules*, 1992, **25**, 290.

166 K. W. Mattison, P. L. Dubin and I. J. Brittain, *J. Phys. Chem. B*, 1998, **102**, 3830.
167 K. R. Grymonpré, B. A. Staggemeier, P. L. Dubin and K. W. Mattison, *Biomacromolecules*, 2001, **2**, 422.
168 E. Seyrek, P. L. Dubin, C. Tribet and E. A. Gamble, *Biomacromolecules*, 2003, **4**, 273.
169 P. M. Biesheuvel and A. Wittemann, *J. Phys. Chem. B*, 2005, **109**, 4209.
170 F. L. B. da Silva, M. Lund, B. Jönsson and T. Åkesson, *J. Phys. Chem. B*, 2006, **110**, 4459.
171 F. L. B. da Silva and B. Jonsson, *Soft Matter*, 2009, **5**, 2862.
172 Y. P. Wen and P. L. Dubin, *Macromolecules*, 1997, **30**, 7856.
173 W. M. de Vos, F. A. M. Leermakers, A. de Keizer, M. A. C. Stuart and J. M. Kleijn, *Langmuir*, 2010, **26**, 249.
174 Y. S. Xu, M. Mazzawi, K. M. Chen, L. H. Sun and P. L. Dubin, *Biomacromolecules*, 2011, **12**, 1512.
175 F. W. Wiegel, *J. Phys. A*, 1977, **10**, 299.
176 C. Y. Kong and M. Muthukumar, *J. Chem. Phys.*, 1998, **109**, 1522.
177 O. A. Evers, G. J. Fleer, J. M. H. M. Scheutjens and J. Lyklema, *J. Colloid Interface Sci.*, 1986, **111**, 446.
178 D. W. Mcquigg, J. I. Kaplan and P. L. Dubin, *J. Phys. Chem.*, 1992, **96**, 1973.
179 H. W. Zhang, K. Ohbu and P. L. Dubin, *Langmuir*, 2000, **16**, 9082.
180 R. Zhang and B. T. Shklovskii, *Physica A*, 2005, **352**, 216.
181 Z. Y. Tang, Y. Wang, P. Podsiadlo and N. A. Kotov, *Adv. Mater.*, 2006, **18**, 3203.
182 F. Bernsmann, B. Frisch, C. Ringwald and V. Ball, *J. Colloid Interface Sci.*, 2010, **344**, 54.
183 V. Kozlovskaya, E. Kharlampieva, M. L. Mansfield and S. A. Sukhishvili, *Chem. Mater.*, 2006, **18**, 328.
184 J. H. Dai, Z. Y. Bao, L. Sun, S. U. Hong, G. L. Baker and M. L. Bruening, *Langmuir*, 2006, **22**, 4274.
185 X. C. Zhou and J. Z. Zhou, *Proteomics*, 2006, **6**, 1415.
186 S. A. Sukhishvili, E. Kharlampieva and V. Izumrudov, *Macromolecules*, 2006, **39**, 8873.
187 T. G. Shutava, D. S. Kommireddy and Y. M. Lvov, *J. Am. Chem. Soc.*, 2006, **128**, 9926.
188 S. Muller, G. Koenig, A. Charpiot, C. Debry, J. C. Voegel, P. Lavalle and D. Vautier, *Adv. Funct. Mater.*, 2008, **18**, 1767.
189 A. Reisch, J. C. Voegel, E. Gonthier, G. Decher, B. Senger, P. Schaaf and P. J. Mesini, *Langmuir*, 2009, **25**, 3610.
190 H. W. Shim, J. H. Lee, T. S. Hwang, Y. W. Rhee, Y. M. Bae, J. S. Choi, J. Han and C. S. Lee, *Biosens. Bioelectron.*, 2007, **22**, 3188.
191 W. S. Tan, R. E. Cohen, M. F. Rubner and S. A. Sukhishvili, *Macromolecules*, 2010, **43**, 1950.
192 I. M. Weidinger, D. H. Murgida, W. F. Dong, H. Mohwald and P. Hildebrandt, *J. Phys. Chem. B*, 2006, **110**, 522.
193 V. Ball, M. Michel, F. Boulmedais, J. Hemmerle, Y. Haikel, P. Schaaf and J. C. Voegel, *Cryst. Growth Des.*, 2006, **6**, 327.
194 R. Spricigo, R. Dronov, F. Lisdat, S. Leimkuhler, F. Scheller and U. Wollenberger, *Anal. Bioanal. Chem.*, 2009, **393**, 225.
195 G. X. Wang, Y. Liu and N. F. Hu, *Electrochim. Acta*, 2007, **53**, 2071.
196 S. T. Milner, *Science*, 1991, **251**, 905.
197 A. Naji, C. Seidel and R. R. Netz, *Adv. Polym. Sci.*, 2006, **198**, 149.
198 E. B. Zhulina and O. V. Borisov, *J. Chem. Phys.*, 1997, **107**, 5952.
199 M. Ballauff and O. Borisov, *Curr. Opin. Colloid Interface Sci.*, 2006, **11**, 316.
200 W. M. de Vos, P. M. Biesheuvel, A. de Keizer, J. M. Kleijn and M. A. Cohen Stuart, *Langmuir*, 2008, **24**, 6575.
201 K. Yoshida and P. L. Dubin, *Colloids Surf., A*, 1999, **147**, 161.
202 E. B. Zhulina and O. V. Borisov, *Langmuir*, 2011, **27**, 10615.
203 F. Carnal and S. Stoll, *J. Phys. Chem. B*, 2011, **115**, 12007.
204 B. Haupt, T. Neumann, A. Wittemann and M. Ballauff, *Biomacromolecules*, 2005, **6**, 948.
205 C. Reichhart and C. Czeslik, *Langmuir*, 2009, **25**, 1047.
206 A. Wittemann and M. Ballauff, *Macromol. Biosci.*, 2005, **5**, 13.
207 K. Henzler, A. Wittemann, E. Breininger, M. Ballauff and S. Rosenfeldt, *Biomacromolecules*, 2007, **8**, 3674.
208 A. Wittemann, B. Haupt and M. Ballauff, *Z. Phys. Chem.*, 2007, **221**, 113.
209 O. V. Borisov, T. M. Birshtein and E. B. Zhulina, *J. Physiol.*, 1991, **1**, 521.
210 F. A. M. Leermakers, M. Ballauff and O. V. Borisov, *Langmuir*, 2007, **23**, 3937.
211 P. Uhlmann, N. Houbenov, N. Brenner, K. Grundke, S. Burkert and M. Stamm, *Langmuir*, 2007, **23**, 57.
212 R. Zimmermann, T. Osaki, T. Kratzmuller, G. Gauglitz, S. S. Dukhin and C. Werner, *Anal. Chem.*, 2006, **78**, 5851.
213 J. Zhou, X. Lu, J. Hu and J. Li, *Chem.–Eur. J.*, 2007, **13**, 2847.
214 P. Jain, J. Dai, S. Grajales, S. Saha, G. L. Baker and M. L. Bruening, *Langmuir*, 2007, **23**, 11360.
215 J. Ladd, Z. Zhang, S. Chen, J. C. Hower and S. Jiang, *Biomacromolecules*, 2008, **9**, 1357.
216 M. T. Bernards, G. Cheng, Z. Zhang, S. F. Chen and S. Y. Jiang, *Macromolecules*, 2008, **41**, 4216.
217 N. Ayres, D. J. Holt, C. F. Jones, L. E. Corum and D. W. Grainger, *J. Polym. Sci., Part A: Polym. Chem.*, 2008, **46**, 7713.
218 E. B. Zhulina and F. A. M. Leermakers, *Soft Matter*, 2009, **5**, 2836.
219 M. Betz, J. Hormansperger, T. Fuchs and U. Kulozik, *Soft Matter*, 2012, **8**, 2477.
220 H. J. Kwon and J. P. Gong, *Curr. Opin. Colloid Interface Sci*, 2006, **11**, 345.
221 H. J. Kwon, Y. Osada and J. P. Gong, *Polym. J.*, 2006, **38**, 1211.
222 C. Gonçalves, P. Pereira and M. Gama, *Materials*, 2010, **3**, 1420.
223 C. Tsitsilianis, *Soft Matter*, 2010, **6**, 2372.
224 S. Lü, M. Liu, B. Ni and C. Gao, *J. Polym. Sci., Part B: Polym. Phys*, 2010, **48**, 1749.
225 Z. Liu, Y. Jiao and Z. Zhang, *J. Appl. Polym. Sci.*, 2007, **103**, 3164.
226 Y. Li, R. d. Vries, M. Kleijn, T. Slaghek, J. Timmermans, M. C. Stuart and W. Norde, *Biomacromolecules*, 2010, **11**, 1754.

227 W. Shi, Y. Ji, X. Zhang, S. Shu and Z. Wu, *J. Pharm. Sci.*, 2011, **100**, 886.
228 B. Stadler, A. D. Price, R. Chandrawati, L. Hosta-Rigau, A. N. Zelikin and F. Caruso, *Nanoscale*, 2009, **1**, 68.
229 A. N. Zelikin, A. D. Price and B. Städler, *Small*, 2010, **6**, 2201.
230 K. T. Oh, T. K. Bronich, V. A. Kabanov and A. V. Kabanov, *Biomacromolecules*, 2006, **8**, 490.
231 K. Kim, J. Cheng, Q. Liu, X. Y. Wu and Y. Sun, *J. Biomed. Mater. Res., Part A*, 2010, **92**, 103.
232 H. G. B. de Jong and H. R. Kruyt, *Proceedings of the Koninklijke Nederlandse Akademie van Wetenschappen*, 1929, **32**, 849.
233 E. Dickinson, *Soft Matter*, 2008, **4**, 932.
234 Y. S. Choi, D. G. Kang, S. Lim, Y. J. Yang, C. S. Kim and H. J. Cha, *Biofouling*, 2011, **27**, 729.
235 L. l. Aberkane, J. Jasniewski, C. Gaiani, J. l. Scher and C. Sanchez, *Langmuir*, 2010, **26**, 12523.
236 H. Lenormand, B. Deschrevel, F. Tranchepain and J. C. Vincent, *Biopolymers*, 2008, **89**, 1088.
237 S. S. Singh, A. K. Siddhanta, R. Meena, K. Prasad, S. Bandyopadhyay and H. B. Bohidar, *Int. J. Biol. Macromol.*, 2007, **41**, 185.
238 Y.-H. Hong and D. J. McClements, *J. Agric. Food Chem.*, 2007, **55**, 5653.
239 S. H. Liu, N. H. Low and M. T. Nickerson, *J. Agric. Food Chem.*, 2009, **57**, 1521.
240 X. Wang, Y.-W. Wang, C. Ruengruglikit and Q. Huang, *J. Agric. Food Chem.*, 2007, **55**, 10432.
241 A. E. Ivanov, L. Nilsson, I. Y. Galaev and B. Mattiasson, *Int. J. Pharm.*, 2008, **358**, 36.
242 H. Dautzenberg, W. Jaeger, J. Kotz, B. Phillip, C. Seidel and D. Stscherbina, *Polyelectrolytes: Formation, Characterization and Application*, Hanser/Gardner Publications, Inc., Cincinnati, 1994.
243 K. Kaibara, T. Okazaki, H. B. Bohidar and P. L. Dubin, *Biomacromolecules*, 2000, **1**, 100.
244 T. Vinayahan, P. A. Williams and G. O. Phillips, *Biomacromolecules*, 2010, **11**, 3367.
245 X. Wang, J. Lee, Y.-W. Wang and Q. Huang, *Biomacromolecules*, 2007, **8**, 992.
246 S. Ulrich, M. Seijo, A. Laguecir and S. Stoll, *J. Phys. Chem. B*, 2006, **110**, 20954.
247 A. Veis, *Adv. Colloid Interf.*, 2011, **167**, 2.
248 J. Gummel, F. Cousin and F. Boue, *J. Am. Chem. Soc*, 2007, **129**, 5806.
249 C. Schmitt and S. L. Turgeon, *Adv. Colloid Interf.*, 2011, **167**, 63.
250 K. J. Klemmer, L. Waldner, A. Stone, N. H. Low and M. T. Nickerson, *Food Chem.*, 2012, **130**, 710.
251 S. Boral and H. B. Bohidar, *J. Phys. Chem. B*, 2010, **114**, 12027.
252 S. G. Anema and C. G. de Kruif, *Soft Matter*, 2012, **8**, 4471.
253 R. J. Stewart, C. S. Wang and H. Shao, *Adv. Colloid Interf.*, 2011, **167**, 85.
254 G. C. Yeo, F. W. Keeley and A. S. Weiss, *Adv. Colloid Interf.*, 2011, **167**, 94.
255 X. Jun-Xia, Y. Hai-yan and Y. Jian, *Food Chem.*, 2011, **125**, 1267.
256 S. Leclercq, C. Milo and G. A. Reineccius, *J. Agric. Food Chem.*, 2009, **57**, 1426.
257 T. K. Kwon and J. C. Kim, *Biomacromolecules*, 2011, **12**, 466.
258 H. Shao, G. M. Weerasekare and R. J. Stewart, *J. Biomed. Mater. Res., Part A*, 2011, **97**, 46.
259 S. M. Hartig, G. Carlesso, J. M. Davidson and A. Prokop, *Biomacromolecules*, 2007, **8**, 265.
260 X. W. Shi, Y. M. Du, L. P. Sun, B. Z. Zhang and A. Dou, *J. Appl. Polym. Sci.*, 2006, **100**, 4614.
261 E. K. F. Yim, A. C. A. Wan, C. Le Visage, I. C. Liao and K. W. Leong, *Biomaterials*, 2006, **27**, 6111.
262 A. Drogoz, S. Munier, B. Verrier, L. David, A. Dornard and T. Delair, *Biomacromolecules*, 2008, **9**, 583.
263 H. L. Jiang, Y. J. Wang, Q. Huang, Y. Li, C. N. Xu, K. J. Zhu and W. L. Chen, *Macromol. Biosci.*, 2005, **5**, 1226.
264 E. K. F. Yim, I. C. Liao and K. W. Leong, *Tissue Eng.*, 2007, **13**, 423.
265 E. Seyrek and P. Dubin, *Adv. Colloid Interf.*, 2010, **158**, 119.
266 L. B. Jaques, *Semin. Thromb. Hemostasis*, 1991, **17**, 1.
267 G. Pavlov, S. Finet, K. Tatarenko, E. Korneeva and C. Ebel, *Eur. Biophys. J.*, 2003, **32**, 437.
268 S. Bertini, A. Bisio, G. Torri, D. Bensi and M. Terbojevich, *Biomacromolecules*, 2005, **6**, 168.
269 X. Guo, M. Condra, K. Kimura, G. Berth, H. Dautzenberg and P. L. Dubin, *Anal. Biochem.*, 2003, **312**, 33.
270 A. D. Lander, *Matrix Biol.*, 1998, **17**, 465.
271 D. J. Johnson, W. Li, T. E. Adams and J. A. Huntington, *EMBO J.*, 2006, **25**, 2029.
272 L. Pellegrini, D. F. Burke, F. von Delft, B. Mulloy and T. L. Blundell, *Nature*, 2000, **407**, 1029.
273 J. Schlessinger, A. N. Plotnikov, O. A. Ibrahimi, A. V. Eliseenkova, B. K. Yeh, A. Yayon, R. J. Linhardt and M. Mohammadi, *Mol. Cell*, 2000, **6**, 743.
274 H. Verli and J. A. Guimaraes, *J. Mol. Graphics Modell.*, 2005, **24**, 203.
275 L. Jin, J. P. Abrahams, R. Skinner, M. Petitou, R. N. Pike and R. W. Carrell, *Proc. Natl. Acad. Sci. U. S. A.*, 1997, **94**, 14683.
276 A. Mushunje, A. Zhou, R. W. Carrell and J. A. Huntington, *Blood*, 2003, **102**, 4028.
277 A. K. Powell, E. A. Yates, D. G. Fernig and J. E. Turnbull, *Glycobiology*, 2004, **14**, 17R.
278 K. R. Catlow, J. A. Deakin, Z. Wei, M. Delehedde, D. G. Fernig, E. Gherardi, J. T. Gallagher, M. S. Pavao and M. Lyon, *J. Biol. Chem.*, 2008, **283**, 5235.
279 J. Kreuger, P. Jemth, E. Sanders-Lindberg, L. Eliahu, D. Ron, C. Basilico, M. Salmivirta and U. Lindahl, *Biochem. J.*, 2005, **389**, 145.
280 N. Jastrebova, M. Vanwildemeersch, A. C. Rapraeger, G. Gimenez-Gallego, U. Lindahl and D. Spillmann, *J. Biol. Chem.*, 2006, **281**, 26884.
281 F. Zhang, X. Liang, D. Pu, K. I. George, P. J. Holland, S. T. Walsh and R. J. Linhardt, *Biochimie*, 2012, **94**, 242.
282 L. S. Jones, B. Yazzie and C. R. Middaugh, *Mol. Cell. Proteomics*, 2004, **3**, 746.

283 M. C. Porfiri, M. Braia, B. Farruggia, G. Picó and D. Romanini, *Process Biochem.*, 2009, **44**, 1046.
284 M. C. Porfiri, G. Picó, B. Farruggia and D. Romanini, *Proc. Biochem.*, 2010, **45**, 1753.
285 V. Boeris, C. Cassane, J. Wagner and G. Picó, *Colloids Surf., B*, 2011, **82**, 354.
286 W. F. Tan, L. K. Koopal, L. P. Weng, W. H. van Riemsdijk and W. Norde, *Geochim. Cosmochim. Acta*, 2008, **72**, 2090.
287 S. Y. Park, R. F. Bruinsma and W. M. Gelbart, *Europhys. Lett.*, 1999, **46**, 454.
288 H. Boroudjerdi and R. R. Netz, *Europhys. Lett.*, 2005, **71**, 1022.
289 H. Schiessel, *Macromolecules*, 2003, **36**, 3424.
290 T. T. Nguyen and B. I. Shklovskii, *J. Chem. Phys.*, 2001, **114**, 5905.
291 A. G. Cherstvy and R. G. Winkler, *Phys. Chem. Chem. Phys.*, 2011, **13**, 11686.
292 R. de Vries, *J. Chem. Phys.*, 2004, **120**, 3475.
293 H.-O. Johansson and J. M. Van Alstine, *Langmuir*, 2006, **22**, 8920.
294 A. B. Kayitmazer, B. Quinn, K. Kimura, G. L. Ryan, A. J. Tate, D. A. Pink and P. L. Dubin, *Biomacromolecules*, 2010, **11**, 3325.
295 D. Andelman and J. F. Joanny, *Macromolecules*, 1991, **24**, 6040.
296 M. Lund and B. Jönsson, *Biochemistry*, 2005, **44**, 5722.
297 K. Giger, R. P. Vanam, E. Seyrek and P. L. Dubin, *Biomacromolecules*, 2008, **9**, 2338.
298 K. Chung, J. Kim, B.-K. Cho, B.-J. Ko, B.-Y. Hwang and B.-G. Kim, *Biochim. Biophys. Acta, Gen. Subj.*, 2007, **1774**, 249.
299 J. S. Mounsey, B. T. O'Kennedy, M. A. Fenelon and A. Brodkorb, *Food Hydrocolloids*, 2008, **22**, 65.
300 N. S. Irina, A. A. Regina, V. S. Mikhail, S. Luciano, I. K. Boris, I. M. Vladimir and A. I. Vladimir, *Macromol. Biosci.*, 2005, **5**, 1184.
301 N. S. Irina, N. N. Irina, S. Luciano, I. M. Vladimir and A. I. Vladimir, *Macromol. Biosci.*, 2007, **7**, 929.
302 S. Stogov, V. Muronets and V. Izumrudov, *Polym. Sci., Ser. C*, 2011, **53**, 97.
303 S. Stogov, V. Izumrudov and V. Muronetz, *Biochemistry*, 2010, **75**, 437.
304 A. Taluja and Y. Bae, *Pharm. Res.*, 2007, **24**, 1517.
305 H. N. Ai Tran, F. Sousa, F. Moda, S. Mandal, M. Chanana, C. Vimercati, M. Morbin, S. Krol, F. Tagliavini and G. Legname, *Nanoscale*, 2010, **2**, 2724.
306 E. Sedlák, D. Fedunová, V. r. Veselá, D. Sedláková and M. n. Antalík, *Biomacromolecules*, 2009, **10**, 2533.
307 W. Park and K. Na, *Biotechnol. Bioprocess Eng.*, 2009, **14**, 668.
308 H. Zhang, A. Saiani, J.-M. Guenet and R. Curtis, *Macromol. Symp.*, 2007, **251**, 25.
309 Y. Lu, A. Wittemann and M. Ballauff, *Macromol. Rapid Comm.*, 2009, **30**, 806.
310 I. Veselova, A. Kireiko and T. Shekhovtsova, *Appl. Biochem. Microbiol.*, 2009, **45**, 125.
311 E. Saburova, S. Tikhonenko, Y. Dybovskaya and B. Sukhorukov, *Russ. J. Phys. Chem. A*, 2008, **82**, 468.
312 V. Boeris, B. Farruggia, B. Nerli, D. Romanini and G. Picó, *Int. J. Biol. Macromol.*, 2007, **41**, 286.
313 A. Marin, D. P. DeCollibus and A. K. Andrianov, *Biomacromolecules*, 2010, **11**, 2268.
314 G. Bassani, B. Farruggia and G. Picó, *Int. J. Biol. Macromol.*, 2011, **49**, 351.
315 V. Boeris, D. Romanini, B. Farruggia and G. Picó, *Process Biochem.*, 2009, **44**, 588.
316 C. Holler and C. Zhang, *Biotechnol. Bioeng.*, 2008, **99**, 902.
317 C. Zhang, R. Lillie, J. Cotter and D. Vaughan, *J. Chromatogr., A*, 2005, **1069**, 107.
318 P. McDonald, C. Victa, J. N. Carter-Franklin and R. Fahrner, *Biotechnol. Bioeng.*, 2009, **102**, 1141.
319 V. Boeris, D. Spelzini, B. Farruggia and G. Picó, *Process Biochem.*, 2009, **44**, 1260.
320 U. K. Aravind, J. Mathew and C. T. Aravindakumar, *J. Membr. Sci.*, 2007, **299**, 146.
321 B. Sarmento, A. J. Ribeiro, F. Veiga, D. C. Ferreira and R. J. Neufeld, *J. Nanosci. Nanotechnol.*, 2007, **7**, 2833.
322 S. J. Shu, X. G. Zhang, D. Y. Teng, Z. Wang and C. X. Li, *Carbohydr. Res.*, 2009, **344**, 1197.
323 I. M. El-Sherbiny, *Carbohydr. Polym.*, 2010, **80**, 1125.
324 C. Johansson, P. Hansson and M. Malmsten, *J. Phys. Chem. B*, 2009, **113**, 6183.
325 S. De Koker, T. Naessens, B. G. De Geest, P. Bogaert, J. Demeester, S. De Smedt and J. Grooten, *J. Immunol.*, 2010, **184**, 203.
326 M. O. Fenley, C. Russo and G. S. Manning, *J. Phys. Chem. B*, 2011, **115**, 9864.